

**Lecture 7) Multidimensional, Self-similar,
strongly-Interacting, Consistent (MuSIC)
Riemann Solvers – Applications to
Divergence-Free MHD**

By

Dinshaw S. Balsara

(dbalsara@nd.edu) Univ. of Notre Dame

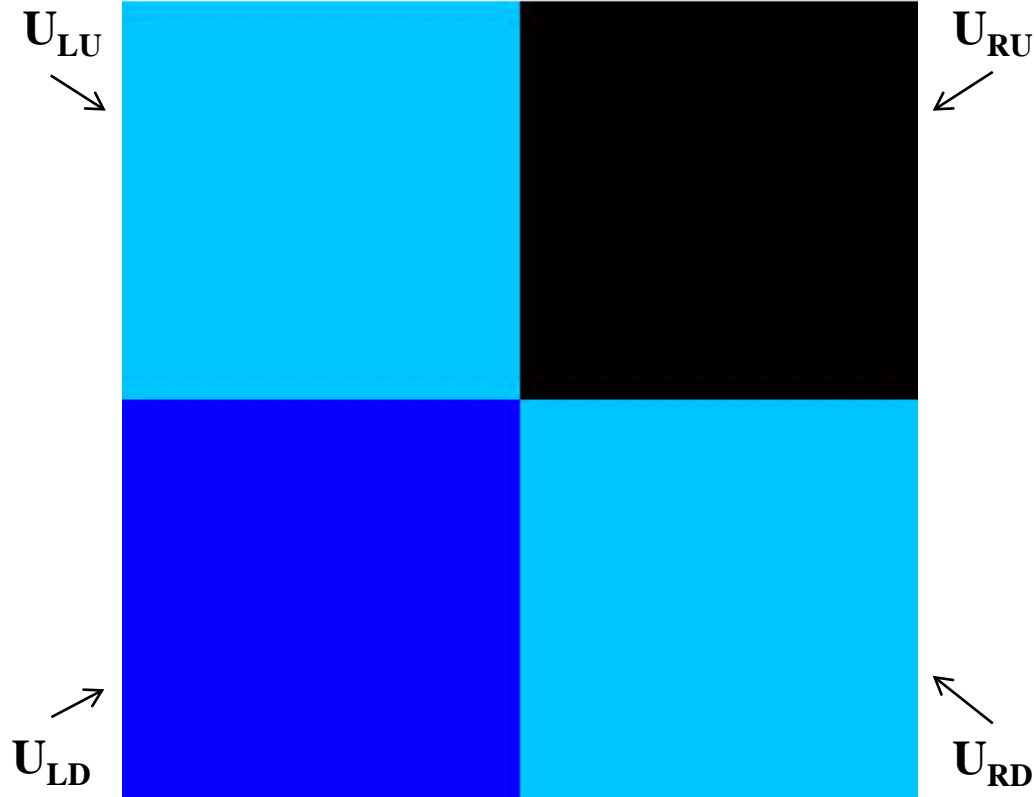
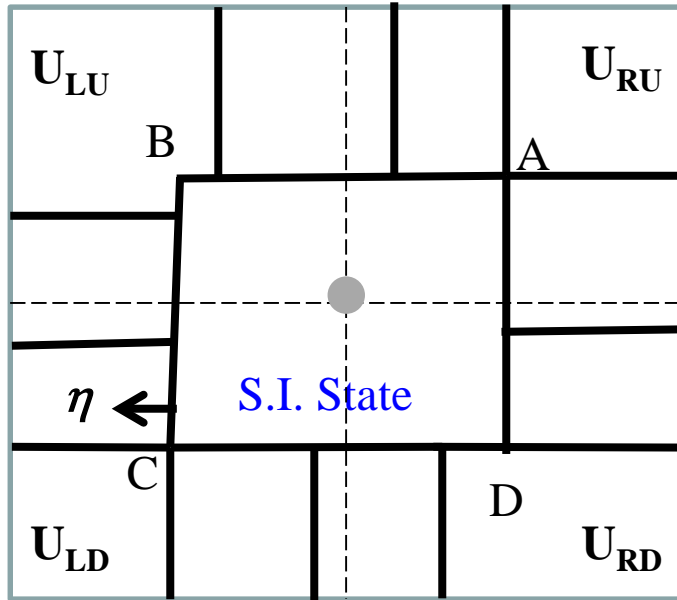
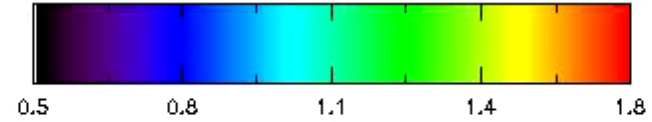
<http://physics.nd.edu/people/faculty/dinshaw-balsara>

<http://www.nd.edu/~dbalsara/Numerical-PDE-Course>



What is the Multidimensional Riemann Problem?

You have always chosen to ignore it!
But it should have been there in your code all along!



How Is It Solved?

MuSIC Riemann solver -- Multidimensional, Self-similar Riemann Solver, based on a strongly-Interacting state that is Consistent with the governing hyperbolic law.

MUSIC Riemann solver -- **M**ultidimensional, **S**elf-similar Riemann Solver, based on a strongly-**I**nteracting state that is **C**onsistent with the governing hyperbolic law. **Four 1D Riemann Problems interact to produce Strongly-Interacting State.**

Note some important properties about the **Strongly-Interacting State**:

- 1) Strongly-Interacting state **evolves self-similarly in space-time.**
- 2) For any **1D RS**, you always build a **1D wave model**. The **strongly-interacting state** is bounded by a **multidimensional wave model**. The multidimensional wave model also evolves **self-similarly in space-time.**
- 3) **Strongly-Interacting state propagates into the four one-dimensional Riemann problems.** I.e., it literally engulfs the fluid in the four one-dimensional Riemann problems that are on all four sides of it. The fluid from those four one-dimensional Riemann problems goes to make up the strongly-interacting state.
- 4) **“In-the-small”** the multidimensional RP **always exists in any code at the vertices of the mesh.** Ignoring multid. effects reduces the timestep.

Overview:-

- 1) Motivating the need for Multidimensional Riemann Solvers using the MHD Equations.
Utility also to ALE Schemes
- 2) Divergence-Free Reconstruction of Magnetic Fields for MHD and AMR-MHD
- 3) Overview of Multidimensional Riemann Solvers – 2D and 3D!
- 4) Formulating the Multidimensional Riemann Solver in Self-Similar Variables
- 5) Approximating the Multidimensional Riemann Problem with just **ONE** call to the Multidimensional Riemann Solver!
- 6) Results and Applications
- 7) Conclusions

Brief Glossary of Recent Work on Multidimensional Riemann Solvers

(Early work – Abgrall 1994a,b, Fey 1998a,b, Brio *et al.* 2001)

Multidimensional HLL Riemann solvers:-

- B. Wendroff, *A two-dimensional HLLC Riemann solver and associated Godunov-type difference scheme for gas dynamics*, Computers and Mathematics with Applications, 38 (1999) 175-185
- D.S. Balsara, *Multidimensional HLLC Riemann solver; Application to Euler and Magnetohydrodynamic Flows*, J. Comput. Phys., 229 (2010) 1970-1993
- J. Vides, B. Nkonga & E. Audit, *A simple two-dimensional extension of the HLLC Riemann solver for gas dynamics*, J. Comput. Phys., 280 (2015) 643-675
- D.S. Balsara, *Three Dimensional HLL Riemann Solver For Conservation Laws on Structured Meshes; Application to Euler and Magnetohydrodynamic Flows*, Journal of Computational Physics 295 (2015) 1

Inclusion of Substructure (Lowers Dissipation):-

- D.S. Balsara, *A two-dimensional HLLC Riemann solver for conservation laws: Application to Euler and magnetohydrodynamic flows*, Journal of Computational Physics 231 (2012) 7476-7503
- D.S. Balsara, *Multidimensional Riemann Problem with Self-Similar Internal Structure – Part I – Application to Hyperbolic Conservation Laws on Structured Meshes*, accepted, Journal of Computational Physics 277 (2014) 163-200
- D.S. Balsara, J. Vides, K. Gurski, B. Nkonga, M. Dumbser, S. Garain, E. Audit, *A Two-Dimensional Riemann Solver with Self-Similar Sub-Structure – Alternative Formulation Based on Least Squares Projection*, Journal of Computational Physics 304 (2016) 138-161

- M. Dumbser and D.S. Balsara, *A New, Efficient Formulation of the HLLEM Riemann Solver for General Conservative and Non-Conservative Hyperbolic Systems*, Journal of Computational Physics 304 (2016) 275-319
- D.S. Balsara , B. Nkonga, M. Dumbser and C.-D. Munz, *Formulating Multidimensional Riemann Solvers in Similarity Variables – Part III :A Multidimensional Analogue of the HLLEM Riemann Solver for Conservative Hyperbolic Systems*, in preparation, Journal of Computational Physics (2016)

Extension to Unstructured Meshes:-

- D.S. Balsara, M. Dumbser and R. Abgrall, *Multidimensional HLL and HLLC Riemann Solvers for Unstructured Meshes – With Application to Euler and MHD Flows*, Journal of Computational Physics 261 (2014) 172-208
- D.S. Balsara and M. Dumbser, *Multidimensional Riemann Problem with Self-Similar Internal Structure – Part II – Application to Hyperbolic Conservation Laws on Unstructured Meshes*, Journal of Computational Physics (2015)

For more information, please see Appendix A from the following website:-

<http://www.nd.edu/~dbalsara/Numerical-PDE-Course>

Applications to ALE:-

- W. Boscheri, D.S. Balsara and M. Dumbser, *Lagrangian ADER-WENO Finite Volume Schemes on Unstructured Triangular Meshes Based on Genuinely Multidimensional HLL Riemann Solvers*, vol. 267, Journal of Computational Physics (2014) Pgs. 112-138
- W. Boscheri, M. Dumbser and D.S. Balsara, *High Order Lagrangian ADER-WENO Schemes on Unstructured Meshes – Application of Several Node Solvers to Hydrodynamics and Magnetohydrodynamics*, to appear, International Journal for Numerical Methods in Fluids, (2014)

Applications to MHD & RMHD:-

- D.S. Balsara, *Divergence-free reconstruction of magnetic fields and WENO schemes for magnetohydrodynamics*, Journal of Computational Physics, 228 (2009) 5040-5056
- D.S. Balsara and M. Dumbser, *Divergence-Free MHD on Unstructured Meshes using High Order Finite Volume Schemes Based on Multidimensional Riemann Solvers*, Journal of Computational Physics 299 (2015) 687-715
- D.S. Balsara and J. Kim, *A Subluminal relativistic Magnetohydrodynamics Scheme with ADER-WENO predictor and multidimensional Riemann solver-based corrector*, Journal of Computational Physics, Vol. 312 (2016) 357-384

Applications to Electromagnetism:-

- D.S. Balsara, T. Amano, S. Garain, J. Kim, *High Order Accuracy Divergence-Free Scheme for the Electrodynamics of Relativistic Plasmas with Multidimensional Riemann Solvers*, to appear, Journal of Computational Physics (2016)

For more information, please see Appendix A from the following website:-

<http://www.nd.edu/~dbalsara/Numerical-PDE-Course>

Advances over Previous Work:-

ANY self-similar 1D Riemann solver can be used as a building block in the Multidimensional Riemann Solver!

Formulation in **Similarity Variables** is easier to understand; especially 3D

Formulation in Similarity Variables is entirely **equivalent** to previous Space-Time Formulation.

Enables seamless inclusion of **sub-structure in the Strongly Interacting State** of the Multidimensional Riemann Problem. The sub-structure can naturally pick out **any orientation w.r.t. mesh** – isotropic propagation.

Galerkin formulation has a plug-and-chug flavor. **Closed form expressions** suitable for applications.

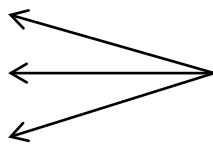
States and Fluxes are **uniquely defined by Integral Constraints**.

Can approximate the Multidimensional Riemann Problem with just **ONE** call to the Multidimensional Riemann Solver!

I) MHD Equations and Motivation:

$$\mathbf{E} \equiv -\mathbf{v} \times \mathbf{B}$$

$$\frac{\partial}{\partial t} \begin{pmatrix} \rho \\ \rho v_x \\ \rho v_y \\ \rho v_z \\ \varepsilon \\ B_x \\ B_y \\ B_z \end{pmatrix} + \frac{\partial}{\partial x} \begin{pmatrix} \rho v_x \\ \rho v_x^2 + P + \mathbf{B}^2/8\pi - B_x^2/4\pi \\ \rho v_x v_y - B_x B_y/4\pi \\ \rho v_x v_z - B_x B_z/4\pi \\ (\varepsilon + P + \mathbf{B}^2/8\pi)v_x - B_x(\mathbf{v} \cdot \mathbf{B})/4\pi \\ 0 \\ (v_x B_y - v_y B_x) \\ -(v_z B_x - v_x B_z) \end{pmatrix}$$


 Hydro + Lorenz Force


 $-\mathbf{E}_z$


 \mathbf{E}_y

$$+ \frac{\partial}{\partial y} \begin{pmatrix} \rho v_y \\ \rho v_x v_y - B_x B_y/4\pi \\ \rho v_y^2 + P + \mathbf{B}^2/8\pi - B_y^2/4\pi \\ \rho v_y v_z - B_y B_z/4\pi \\ (\varepsilon + P + \mathbf{B}^2/8\pi)v_y - B_y(\mathbf{v} \cdot \mathbf{B})/4\pi \\ 0 \\ -(v_x B_y - v_y B_x) \\ (v_y B_z - v_z B_y) \end{pmatrix} + \frac{\partial}{\partial z} \begin{pmatrix} \rho v_z \\ \rho v_x v_z - B_x B_z/4\pi \\ \rho v_y v_z - B_y B_z/4\pi \\ \rho v_z^2 + P + \mathbf{B}^2/8\pi - B_z^2/4\pi \\ (\varepsilon + P + \mathbf{B}^2/8\pi)v_z - B_z(\mathbf{v} \cdot \mathbf{B})/4\pi \\ (v_z B_x - v_x B_z) \\ -(v_y B_z - v_z B_y) \\ 0 \end{pmatrix} = 0$$


 \mathbf{E}_z


 $-\mathbf{E}_x$


 $-\mathbf{E}_y$


 \mathbf{E}_x

Notice the dualism between the flux terms and the electric field

MHD Is Different: $\frac{\partial \mathbf{B}}{\partial t} + c \nabla \times \mathbf{E} = 0$; $\mathbf{E} \equiv -\frac{1}{c} \mathbf{v} \times \mathbf{B}$; constraint $\nabla \cdot \mathbf{B} = 0$

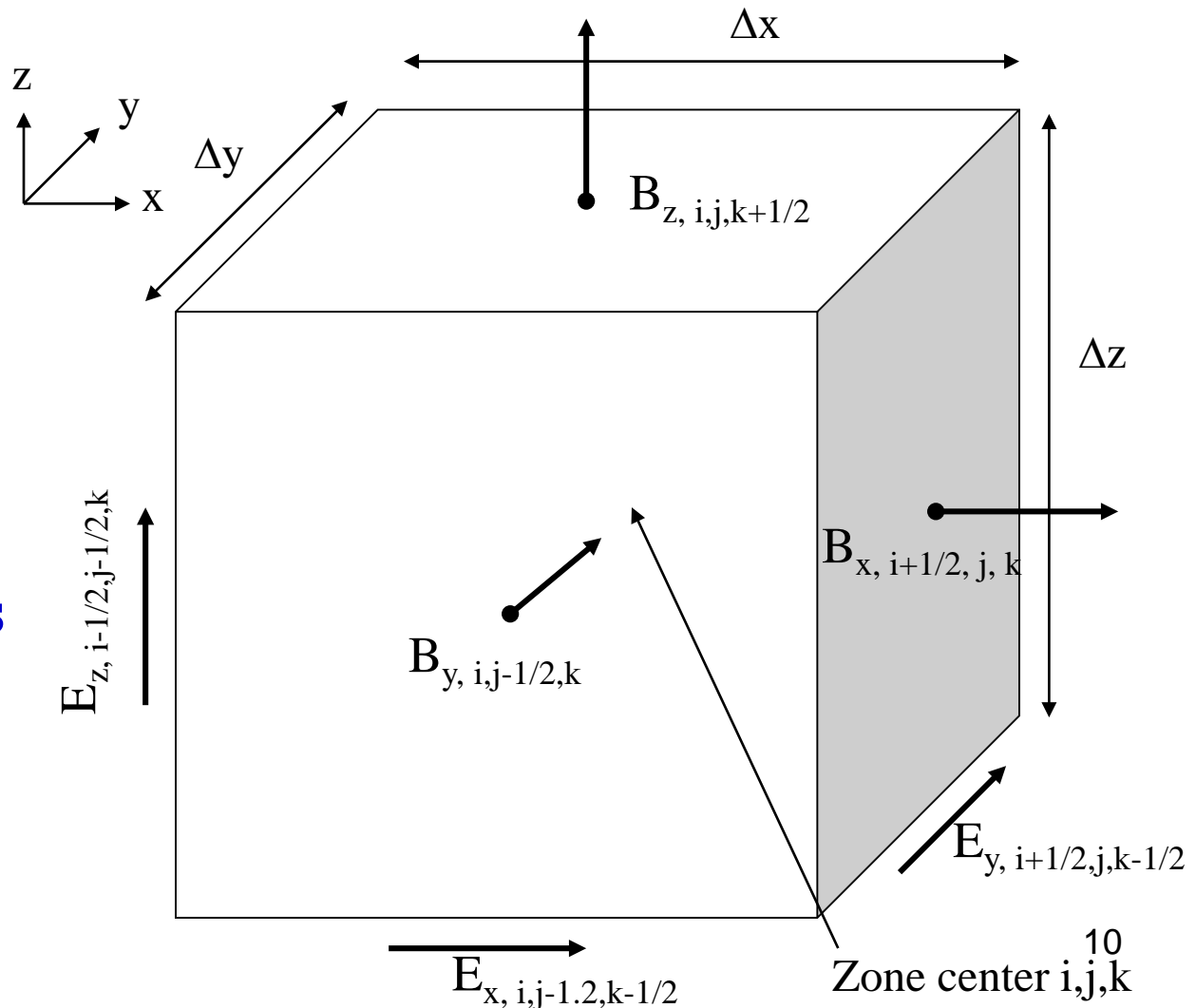
Necessitates use of Yee-type mesh. Fluid variables still zone-centered.

Magnetic field components at zone faces; electric fields at zone edges.

Since \mathbf{B} is defined on faces, we need a reconstruction of \mathbf{B} over the zone that respects the constraint:

$$\nabla \cdot \mathbf{B} = 0!$$

Electric fields at edges require genuinely multi-d treatment – Need for at least genuinely 2D Riemann Solvers



There is a **dualism between the fluxes** of the conservation law **and the electric field** (Balsara & Spicer 1999). That can be exploited to obtain the electric field.

For this concept to truly work, the **electric field** should be treated **truly multidimensionally**.

All prior work had tried combinations of 1D RP to introduce multidimensionality into the electric field evaluation.

There was even an attempt to stabilize the electric field by doubling the dissipation (Gardiner&Stone 2005). **Why double dissipation all the time?**

Any doubling of dissipation proves to be **completely unnecessary** when the **genuinely Multidimensional Riemann solvers** are used to obtain the edge-centered electric field (Balsara 2010, 2012, 2014).

Essential ideas:

Div-Free Reconstruction +

Dualism of fluxes and E-field + true multidimensional RS

Motivation for Divergence-Free Reconstruction of Magnetic Fields

Why have Divergence-Free MHD Reconstruction?

- 1) **Divergence-cleaning** strategies (Brackbill & Barnes) run into problems. There are often modes that the divergence-cleaning routines do not remove (Balsara & Kim 2004).
- 2) **Powell (1994) fix** destroys the **conservation form** of the MHD system. Requires very substantial modification of the Riemann solvers.
 - Also results in **accumulation of divergence** at stagnation points.
- 3) **GLM** formulation by Dedner et al (2002) require an **a priori** evaluation of the **extremal speed**. In most real-world applications, such a speed is not available. Try any magnetospheric problem, any astrophysics problem or any fusion problem!
 - Low dissipation **HLL, HLLC, HLLD RS are hard to design** when the extremal speeds belong to the lagrange multiplier field.
 - **Linearized RS not very successful** for MHD.
- 4) For **closed/periodic geometries**, the divergence never goes away.

Motivation for Multidimensional Riemann Solvers

Why have multidimensional Riemann solvers?

- 1) For **divergence-free MHD**, the motivation is especially compelling: There is no unique mesh-oriented direction for the **edge-centered electric field**. Electric field evaluation is fundamentally **multidimensional**.
- 2) Better representation of the physics. Astrophysical, space science, AME and fusion calculations are carried out on **resolution-starved meshes**. Multidimensional Riemann solvers give more **isotropic propagation of small-scale flow features**.
- 3) Multidimensional effects in fluxes → **larger timesteps; larger CFL**.
- 4) Multidimensional Riemann solvers are **cost-competitive** with 1d Riemann solver technology.
- 5) Extended now to **unstructured meshes** and **ALE** formulations.

II) Divergence-Free Methods in MHD & AMR-MHD

MHD is different, Reason: The magnetic field evolves according to Faraday's law, i.e. a Stokes-law type update equation.

$$\frac{\partial \mathbf{B}}{\partial t} + c \nabla \times \mathbf{E} = 0 ; \quad \mathbf{E} = -\frac{1}{c} \mathbf{v} \times \mathbf{B}$$

Which satisfies the constraint: $\nabla \cdot \mathbf{B} = 0$

Violating this constraint results in unphysical forces along the magnetic field.

Numerical methods for satisfying the constraint exist and rely on a staggered mesh formulation. Yee (1966), Brecht et al (1981)

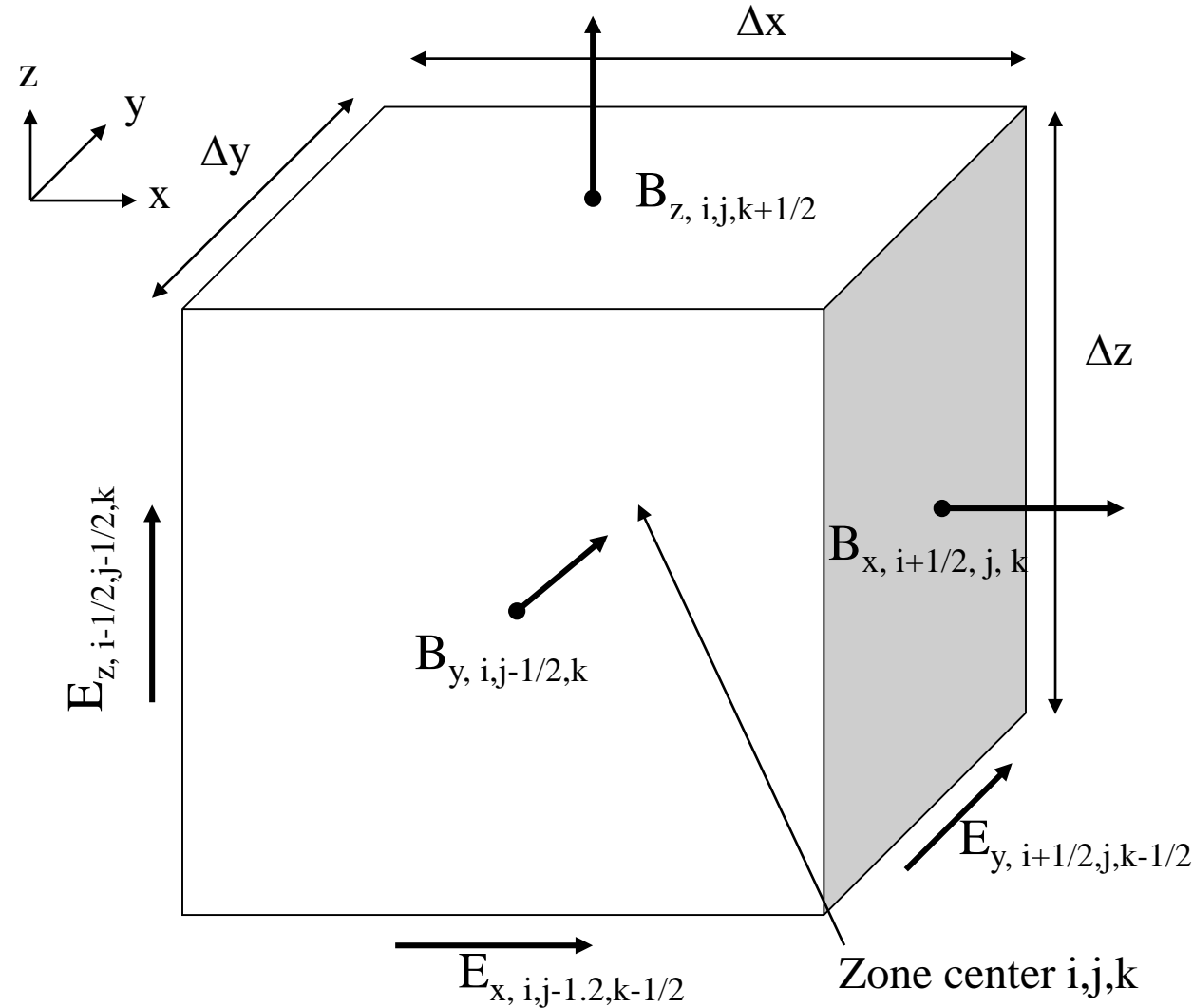
The magnetic field components are defined at the face centers.

The electric field components are defined at the edge centers.

Notice: Face-centered magnetic fields are the fundamental quantity!

$$\frac{\partial \mathbf{B}}{\partial t} + c \nabla \times \mathbf{E} = 0 ; \quad \nabla \cdot \mathbf{B} = 0$$

$$\Rightarrow \mathbf{B}_{x, i+1/2, j, k}^{n+1} = \mathbf{B}_{x, i+1/2, j, k}^n - \frac{c \Delta t}{\Delta y \Delta z} \begin{pmatrix} \Delta z E_{z, i+1/2, j+1/2, k}^{n+1/2} - \Delta z E_{z, i+1/2, j-1/2, k}^{n+1/2} \\ + \Delta y E_{y, i+1/2, j, k-1/2}^{n+1/2} - \Delta y E_{y, i+1/2, j, k+1/2}^{n+1/2} \end{pmatrix}$$



Important Questions:

1) How do we reconstruct the magnetic field if it resides on the boundaries?

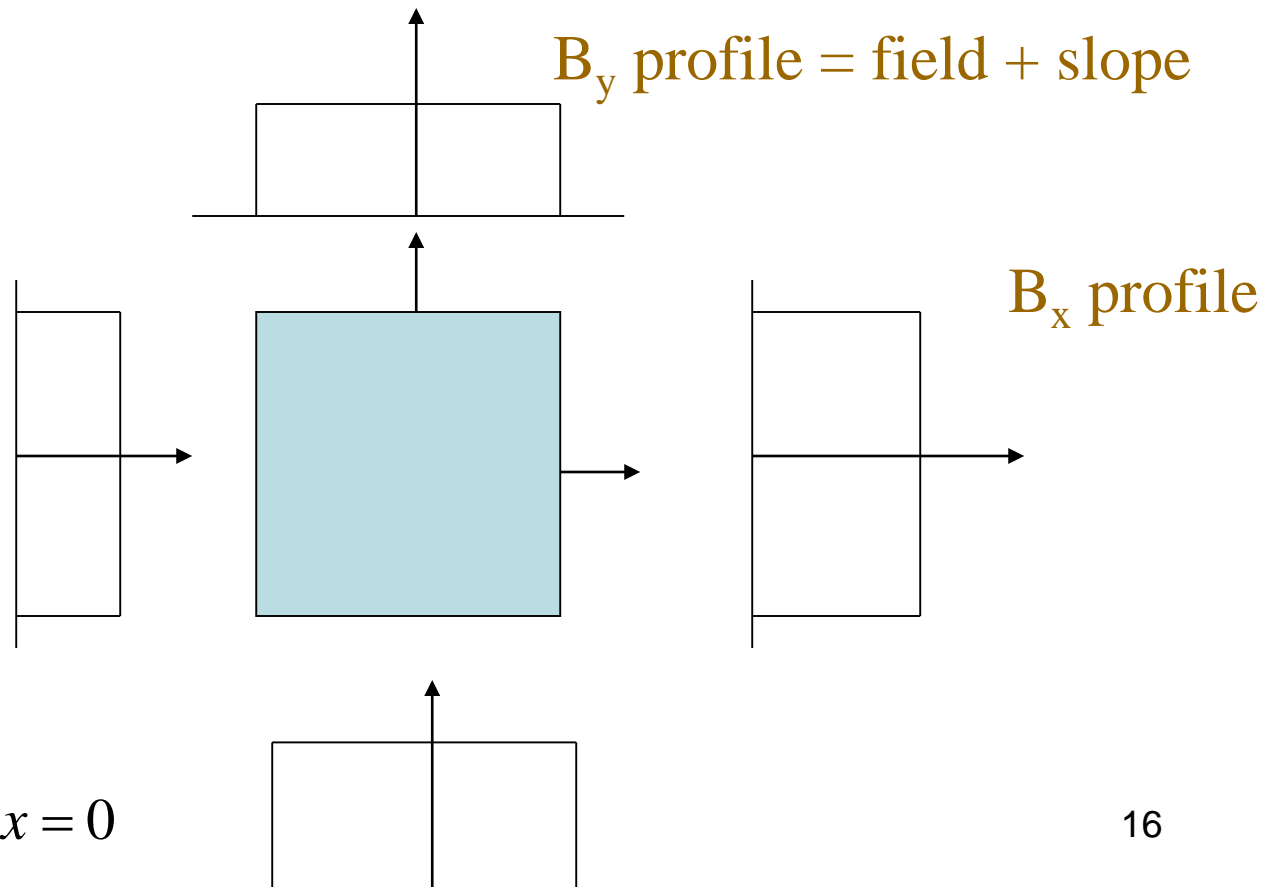
2) How do we obtain upwinded electric fields?

Divergence-Free Prolongation / Reconstruction of B-Field

Start with magnetic fields at faces in 2D – This is only first order accurate.

This will only give us first order accuracy. We wish to have at least second order, so we endow the fields with linear variation.

Count: Boundaries have
3 independent pieces
of information!



Divergence-free
Constraint →

$$(B_x^+ - B_x^-) \Delta y + (B_y^+ - B_y^-) \Delta x = 0$$

Divergence-Free Prolongation / Reconstruction of B field

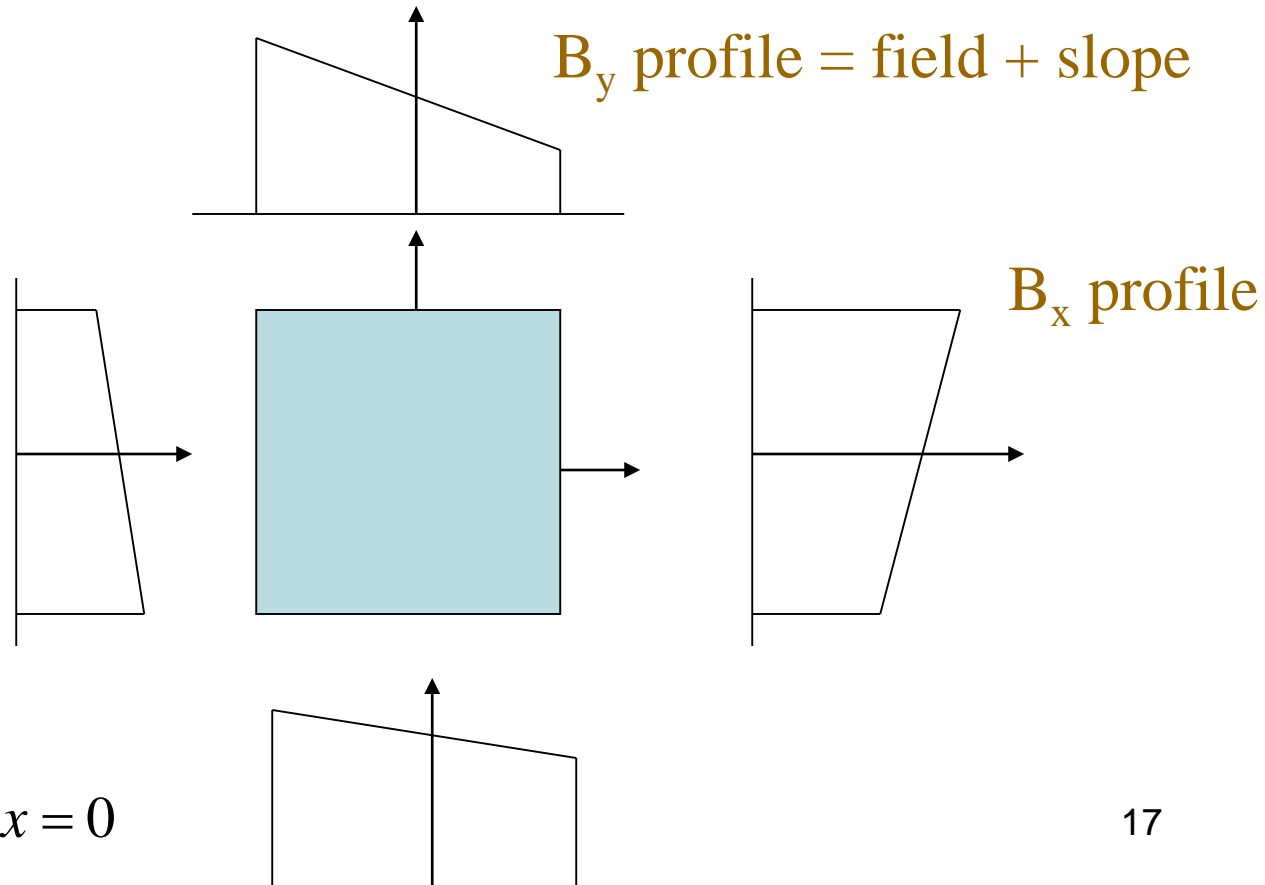
Fields defined at mesh faces are endowed with linear profiles for 2nd order accuracy. (Just like fluid slabs having linear profiles.)

Reconstruction → Find the **Divergence-free polynomial** in the *interior* of the (coarse) zone so that it matches the linear profiles at the *boundaries* :-

Count: Boundaries have
7 independent pieces
of information!

Divergence-free
Constraint →

$$(B_x^+ - B_x^-) \Delta y + (B_y^+ - B_y^-) \Delta x = 0$$

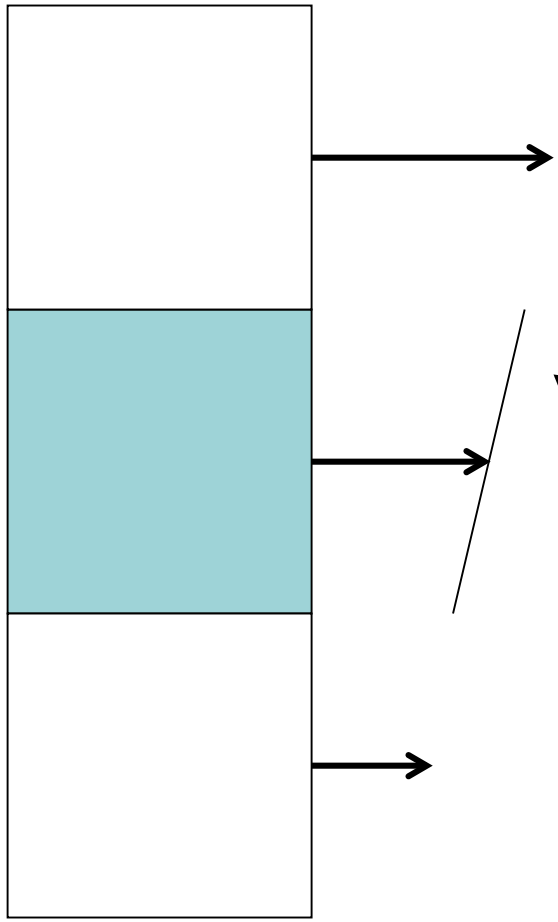


How do we obtain the facial variation in the field?

Focus on 2nd order, piecewise linear reconstruction

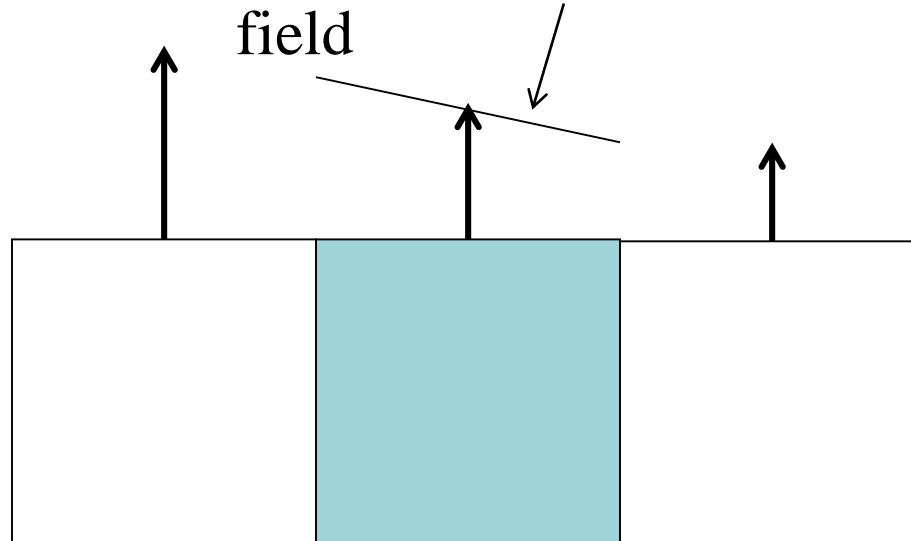
For a structured mesh, this is easy.

For an unstructured mesh, it is only a little more difficult.



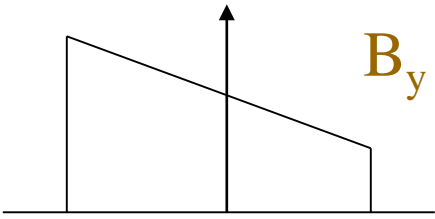
Limit in vertical direction to obtain slope in y-direction for the x-magnetic field.

Limit in the horizontal direction to obtain Slope in the x-direction for the y-magnetic field

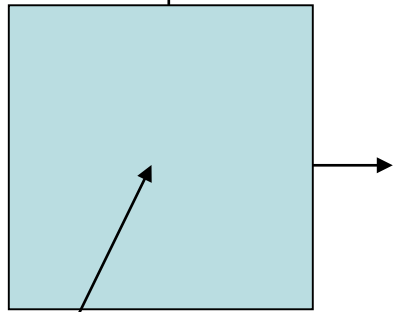
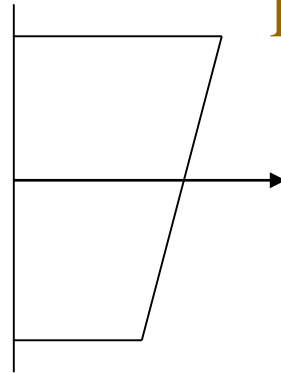


1 Divergence-free constraint:-

B_y profile = field + slope



B_x profile



$$B_x(x,y) = a_0 + a_x x + a_y y$$

$$B_y(x,y) = b_0 + b_x x + b_y y$$

$$\partial_x B_x(x,y) + \partial_y B_y(x,y) = 0$$

$$\Rightarrow a_x + b_y = 0 ;$$

First try: Use only piecewise linear profiles for B.

Clearly, we need more terms in the polynomial....

3 Divergence-free constraints:-

$$\partial_x B_x(x,y) + \partial_y B_y(x,y) = 0$$

$$\Rightarrow a_x + b_y = 0 ;$$

$$2 a_{xx} + b_{xy} = 0 ;$$

$$a_{xy} + 2 b_{yy} = 0$$

B_y profile = field + slope

B_x profile

10 polynomial Coefficients; contain *all* needed *2nd order terms + more (underlined)*

$$B_x(x,y) = a_0 + a_x x + a_y y + \underline{a_{xx} x^2 + a_{xy} x y}$$

$$B_y(x,y) = b_0 + b_x x + b_y y + \underline{b_{xy} x y + b_{yy} y^2}$$

Count!: 3 (fields) + 4 (slopes) = 7 = 10 (coefficients) – 3 (constraints)

While demonstrated for second order on rectangles, this process *can be carried out for all orders for cubes and tetrahedra.*

Divergence-free reconstruction in 3d is a little more intricate. But it has been done in Balsara (2001), Balsara (2004).

Higher order reconstruction, up to fourth order, leading to higher order divergence-free MHD schemes have been done in Balsara (2009).

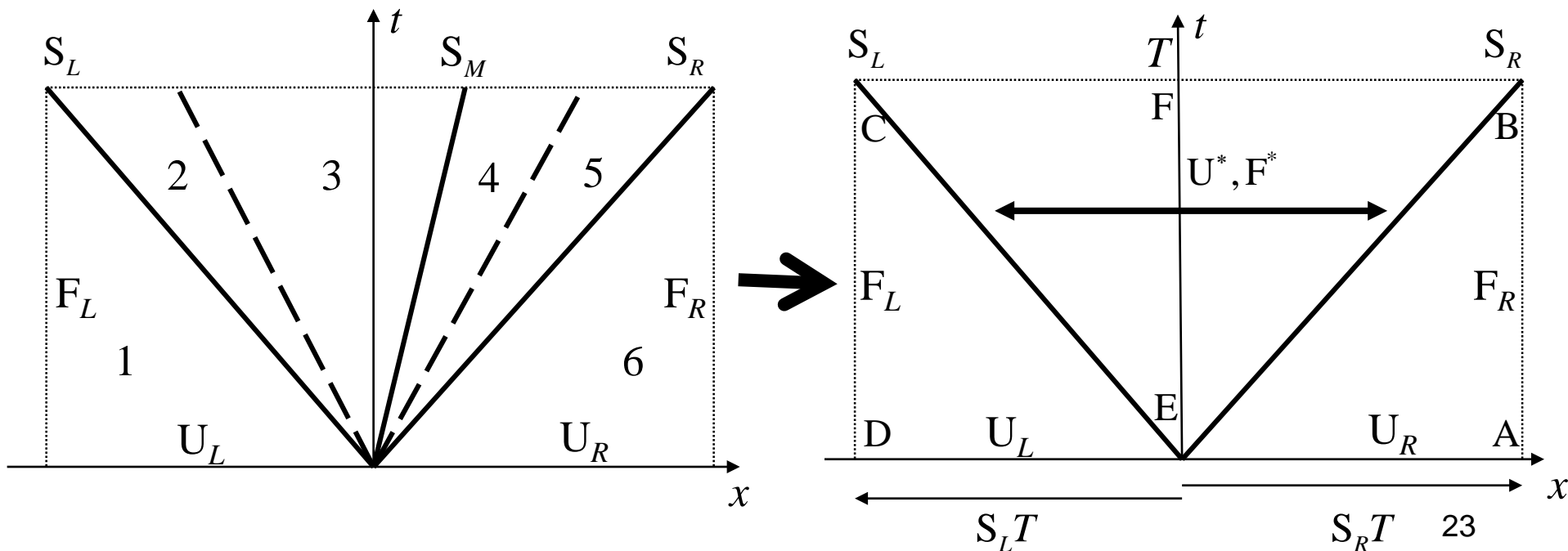
Divergence-free AMR-MHD schemes also presented in Balsara (2001).

Extension to unstructured meshes has also been done recently by Balsara & Dumbser (2015) and Xu, Balsara & Du (2016).

Many of the details produced by a Riemann solver (RS) are never used in a computer code.

Motivates need for an *approximate Riemann solver* – topic of this talk. See fig. below. The approximate RS has to satisfy some requirements:

- 1) A *self-similar wave model* in space-time.
- 2) *Consistency* with the conservation law, $\partial_t \mathbf{U} + \partial_x \mathbf{F} = 0$. Gives \mathbf{U}^* & \mathbf{F}^* !
- 3) *Entropy enforcement*. Provide dissipation at rarefaction fans.
- 4) V. Desirable but not essential: Preservation of *internal sub-structures*.



Exact Riemann Solver

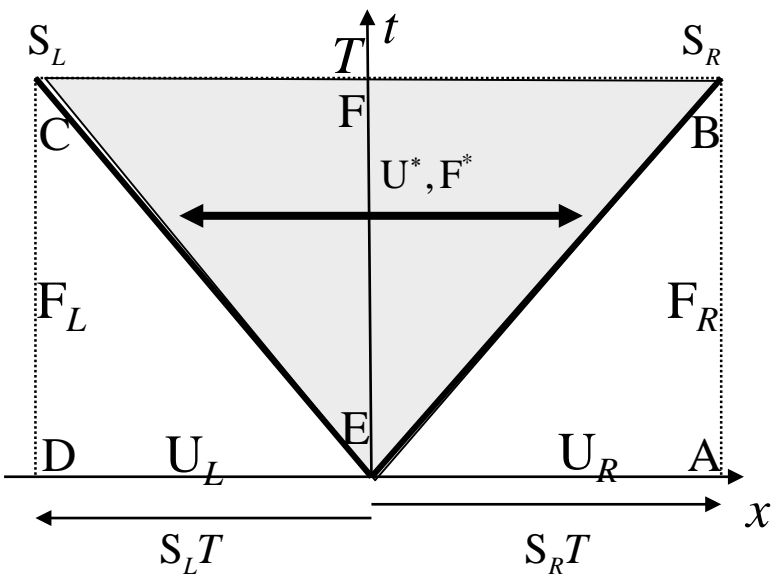
Approximate HLL Riemann Solver

Previous slides only described the 1d situation. Obtaining the strongly-interacting subsonic state U^* , and associated flux F^* , was of interest there.

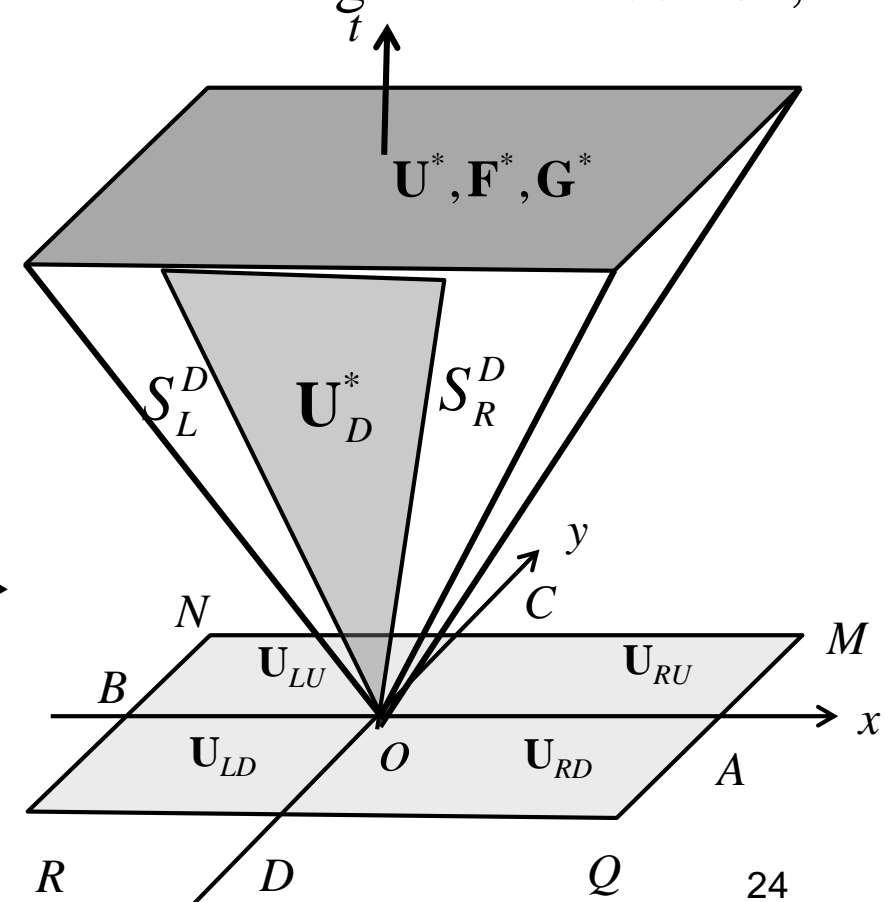
We will only see **multidimensional effects** at the **vertices** of a mesh.

It is desirable to introduce **multi-dimensional effects** in order to get more consistency with the physics. When 4 states come together at a **vertex**; we have a **multi-dimensional RP**.

Two space + 1 time dimension.



1D HLL RS: 1 space + 1 time



2D HLL RS: 2 space + 1 time

Wave model changes:- **Inverted triangle** → **Inverted Pyramid** –

Contains the Strongly-Interacting state:-

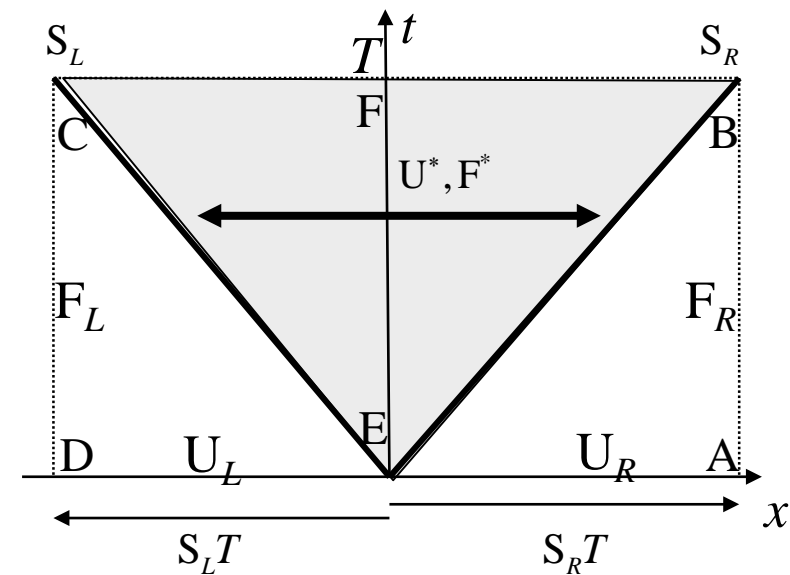
(Two-dimensional SI state is formed by eating into the 1D RP solutions.)

1) Strongly-Interacting state evolves **self-similarly**. Reduces to 1D RP in limit where flow is one-dimensional – notice the 1D RP in side panels.

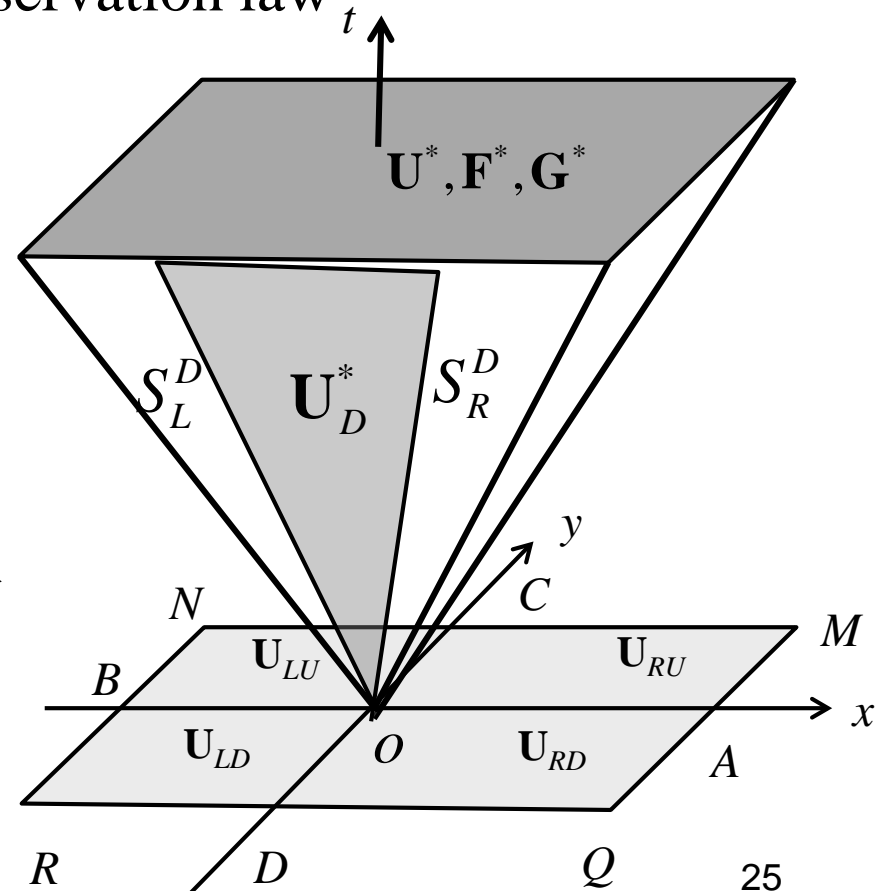
2) \mathbf{U}^* , \mathbf{F}^* , \mathbf{G}^* are obtained from 2D conservation law

$$\partial_t \mathbf{U} + \partial_x \mathbf{F} + \partial_y \mathbf{G} = 0 \quad \text{via } \mathbf{consistency}.$$

3) If inverted pyramid is wide enough, we get **entropy enforcement in 2D!**



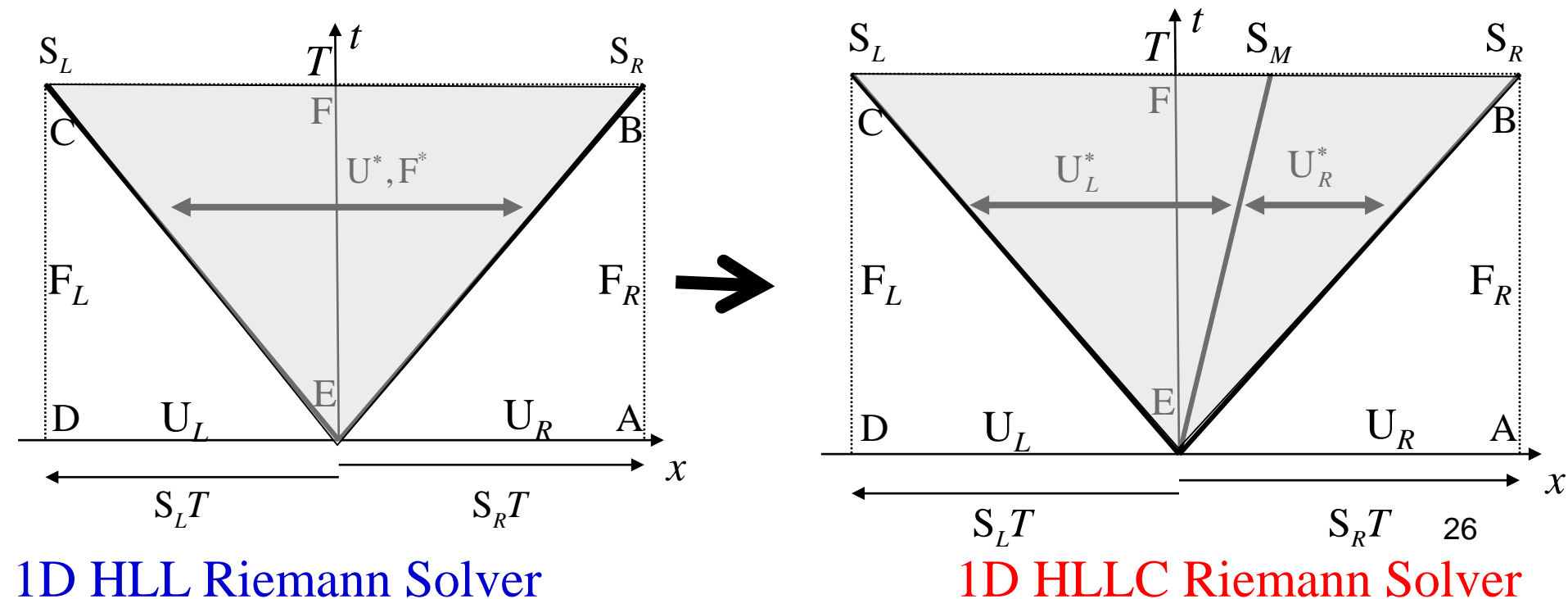
1D HLL RS: 1 space + 1 time



2D HLL RS: 2 space + 1 time

The 1D and 2D HLL Riemann solvers, shown previously, average over important internal sub-structures in the RP. Specifically, the **contact discontinuity** is smeared.

The **HLLC/HLLD/linearized Riemann solvers** are approximate RS that restore the sub-structure back into the Riemann problem. See below.



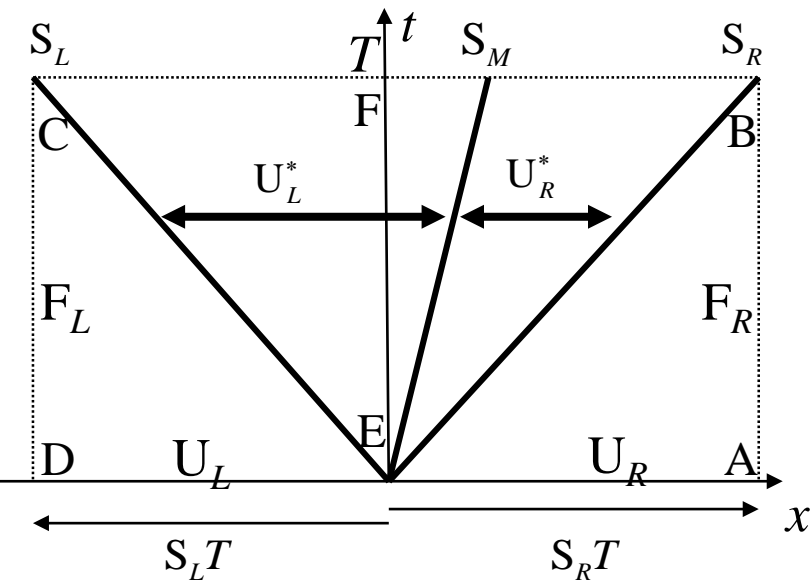
1D HLL Riemann Solver

1D HLLC Riemann Solver

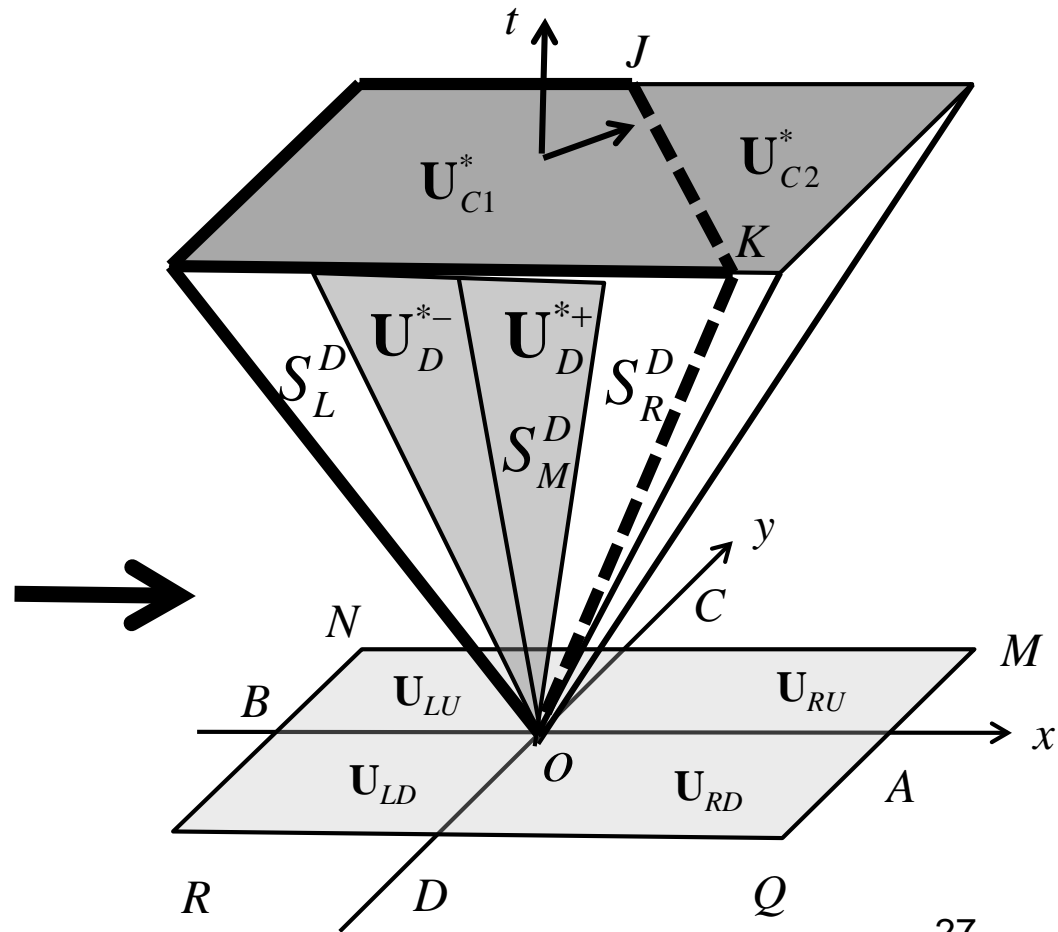
Restoring the contact discontinuity in multi-dimensions is highly desirable. It permits flow structures to propagate isotropically in all directions relative to the mesh. CD moves at any angle w.r.t. mesh.

Restoring the contact discontinuity has been done in Balsara (2012), BDA14.

Supersonic cases are easy.



1D HLLC RS

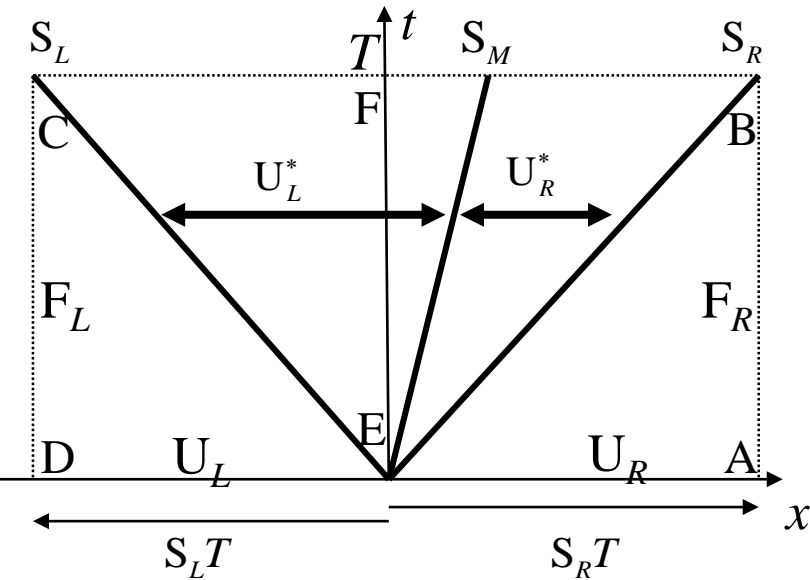


2D HLLC RS with Contact

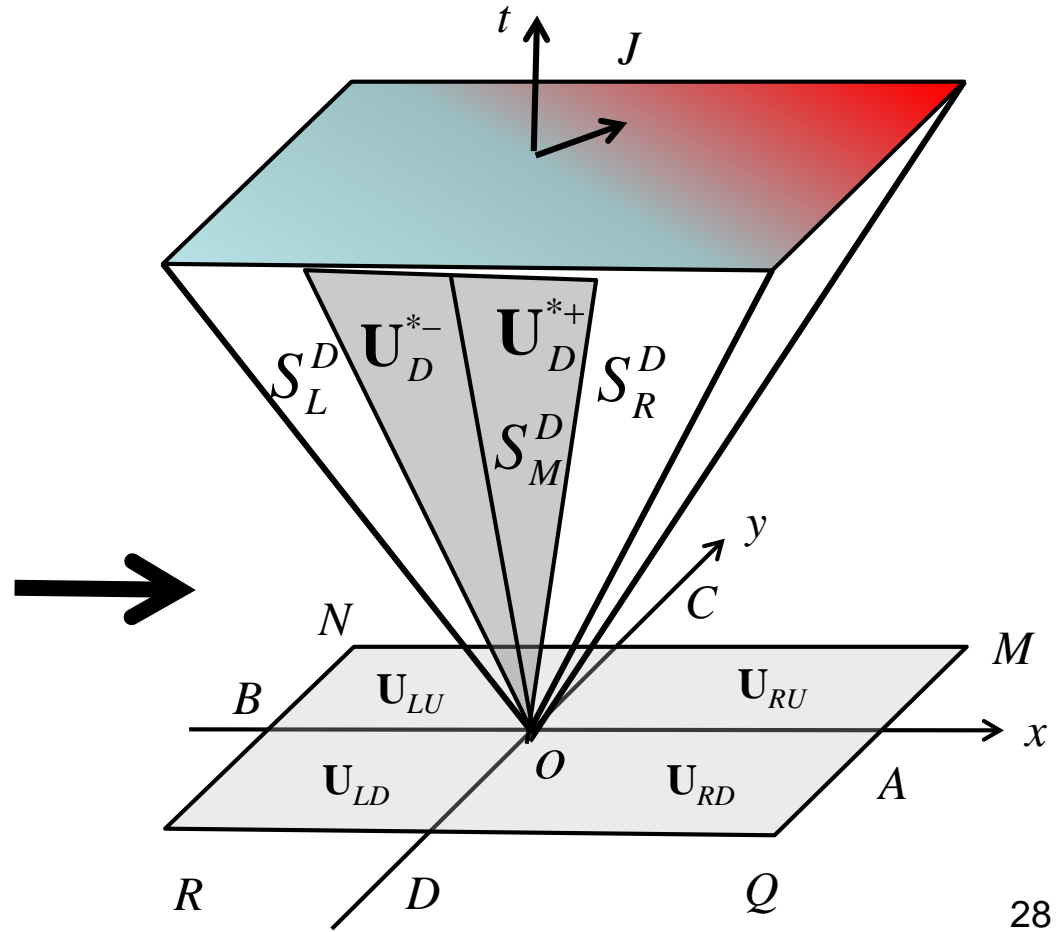
Restoring the sub-structure in multi-dimensions is highly desirable. It permits flow features to propagate isotropically in all directions relative to the mesh. Sub-structure can be at any angle w.r.t. mesh.

Restoring the general sub-structure has been done in Balsara (2014).

Supersonic cases are easy.



1D HLLC RS

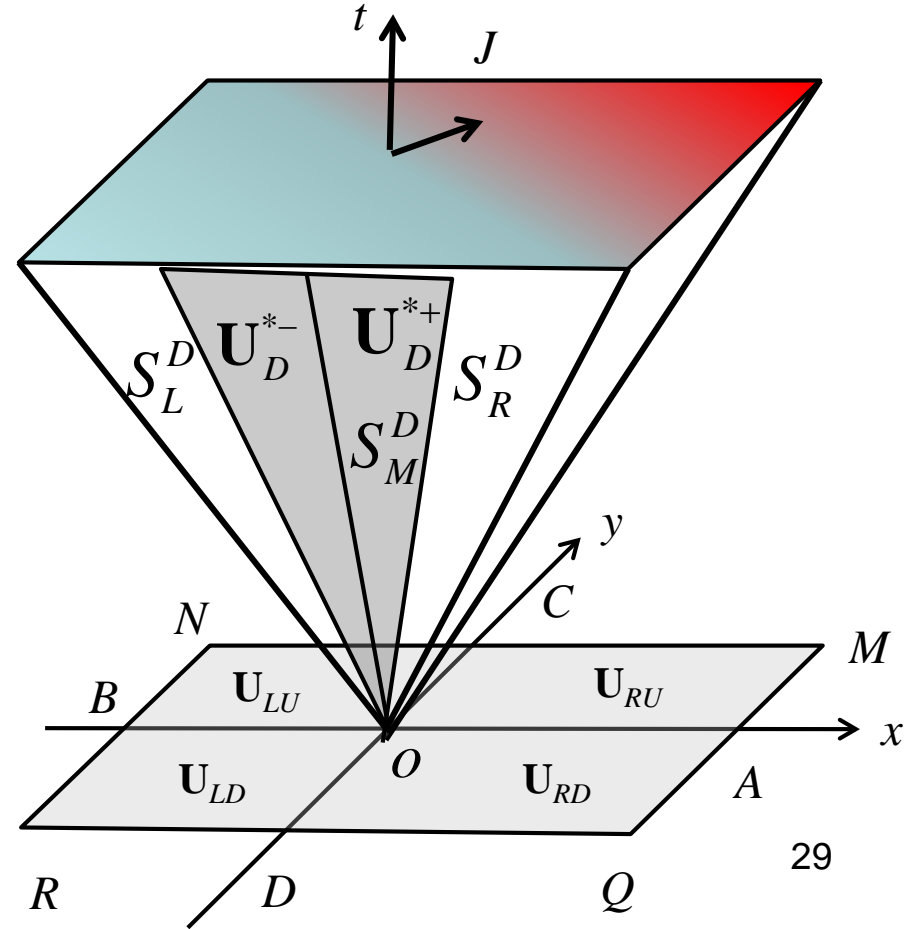
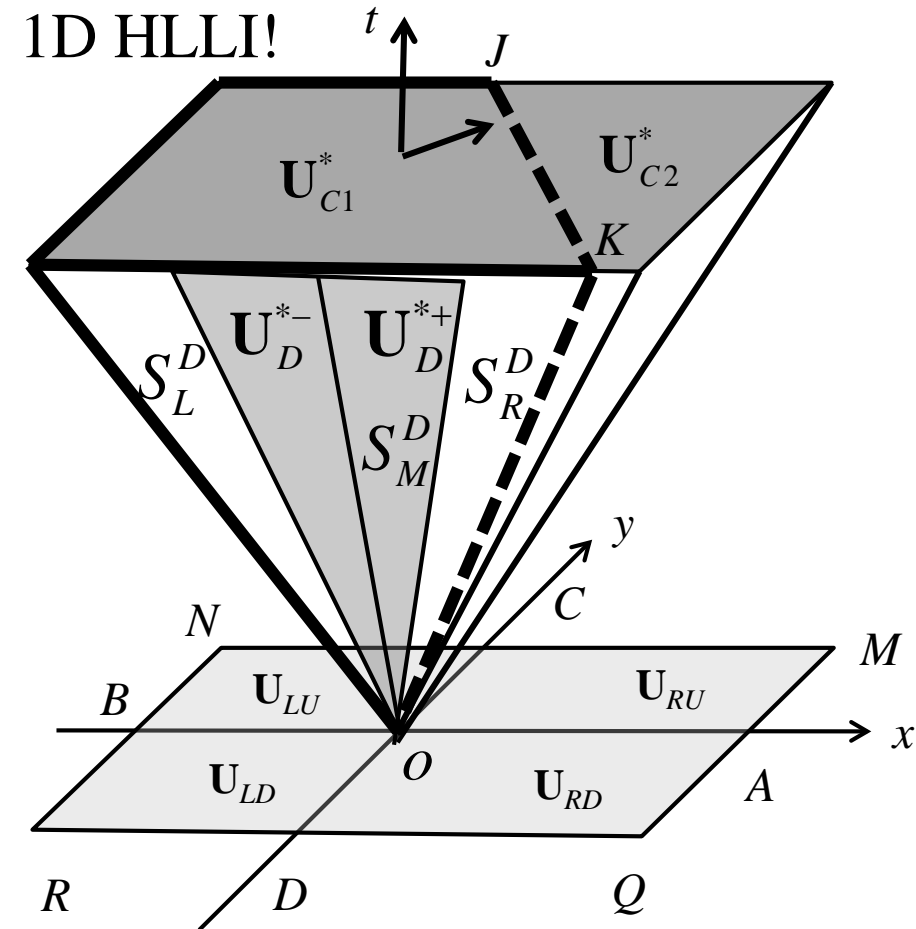


2D RS with Sub-structure

When flow features/shocks are **mesh-aligned** (on logically rectangular meshes) the 2D Riemann Solver **reduces exactly to the 1D RS!**

The flat panels in the construction of the RS ensure that this happens. It explains why the wave model was chosen to have **flat panels** on its sides.

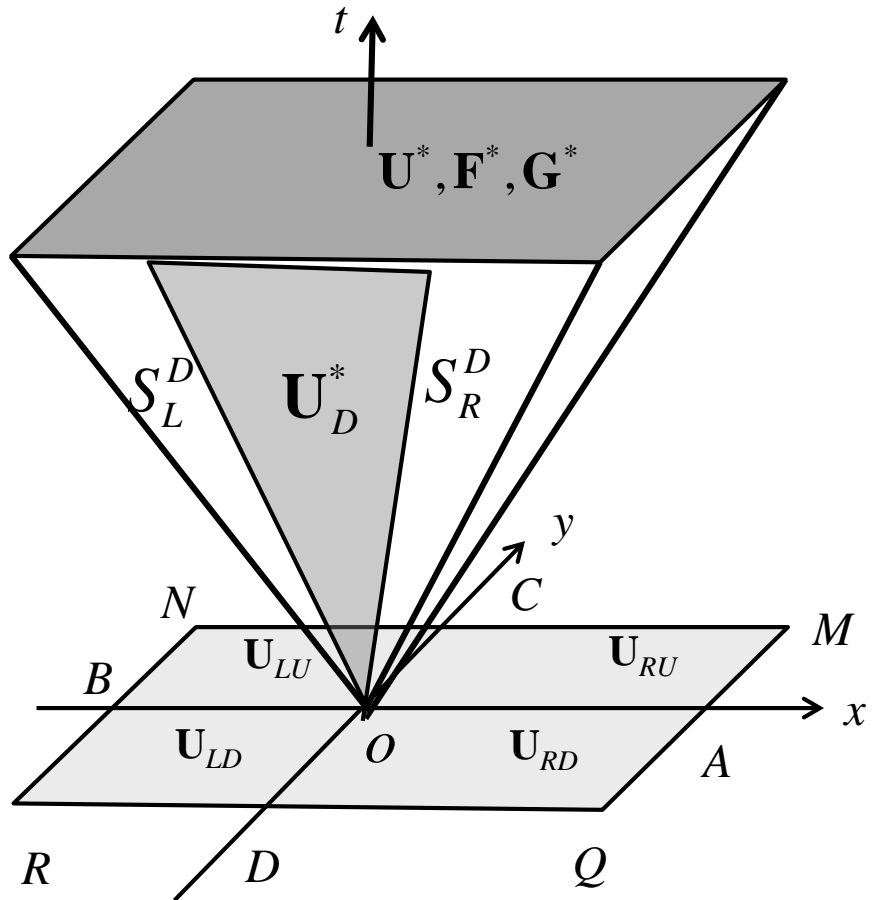
The 2D HLLC reduces to 1D HLLC; the self-similar 2D RS reduces to 1D HLLI!



From Space-Time to Self-Similar Variables: The space-time approach is very difficult to extend to three dimensions. That is why we invented the self-similarity variables. It **reduces the dimensionality of the problem** by casting the variables in terms of **speed of propagation**.

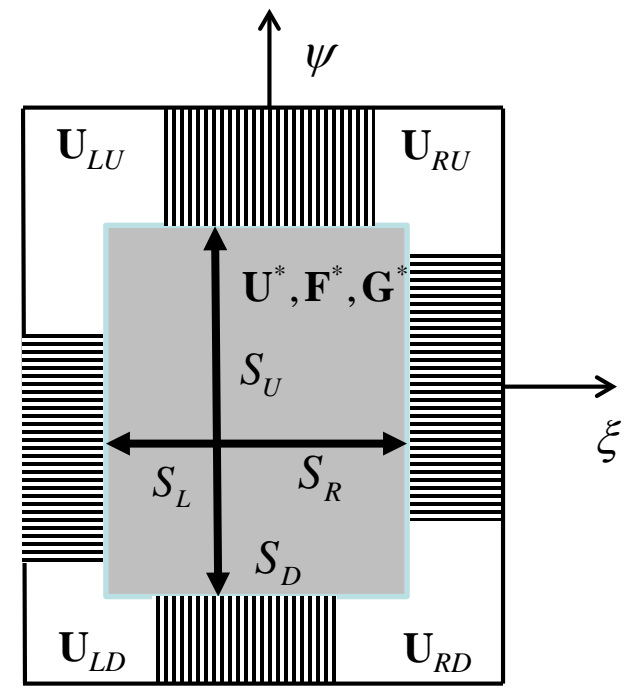
Space-Time Picture

Variables in 2D : x, y, t



Picture in **Self-Similar Variables**

Variables in 2D : $\xi \equiv \frac{x}{t}, \quad \psi \equiv \frac{y}{t}$

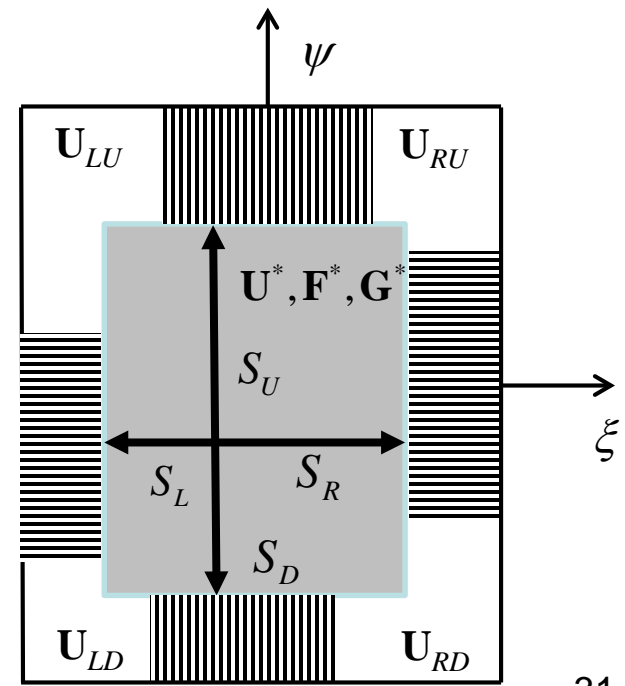
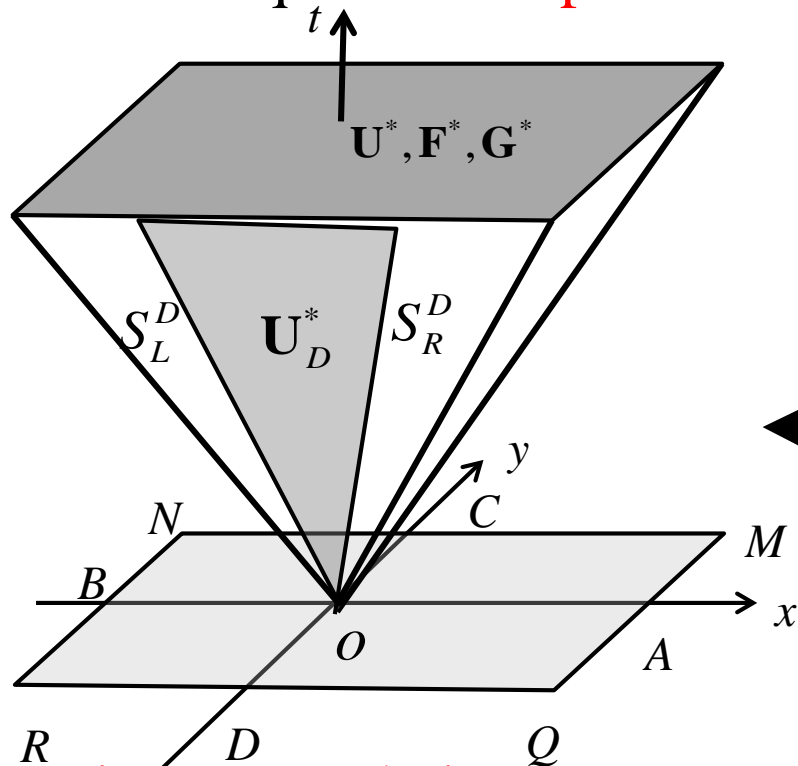


Formulation in similarity variables equivalent to space-time formulation!

The constant state U^* now becomes the **region of strong interaction U^*** .

Because of *self-similarity*, the constant state U^* forms an **inverted pyramid with polygonal base in a 3D space-time**. Seen from the top, the pyramid is a rectangle.

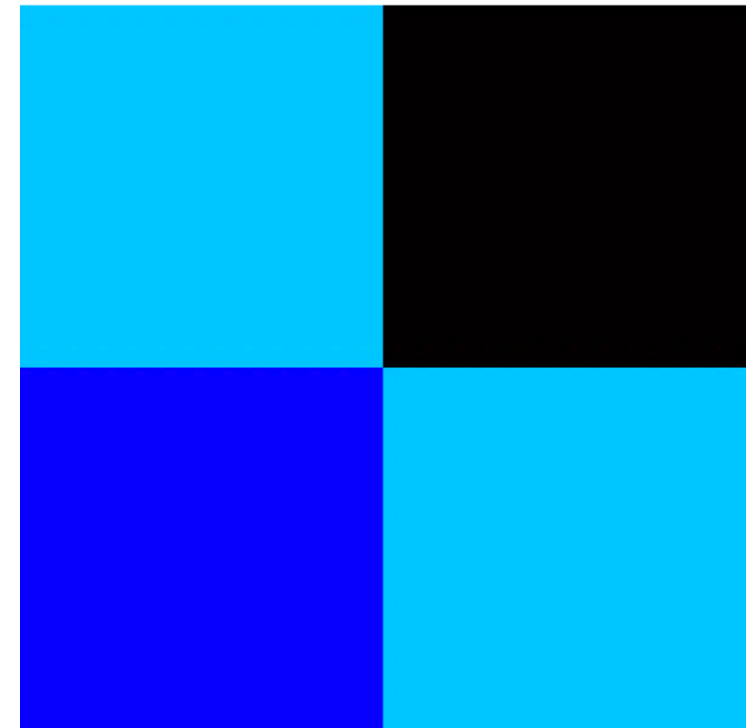
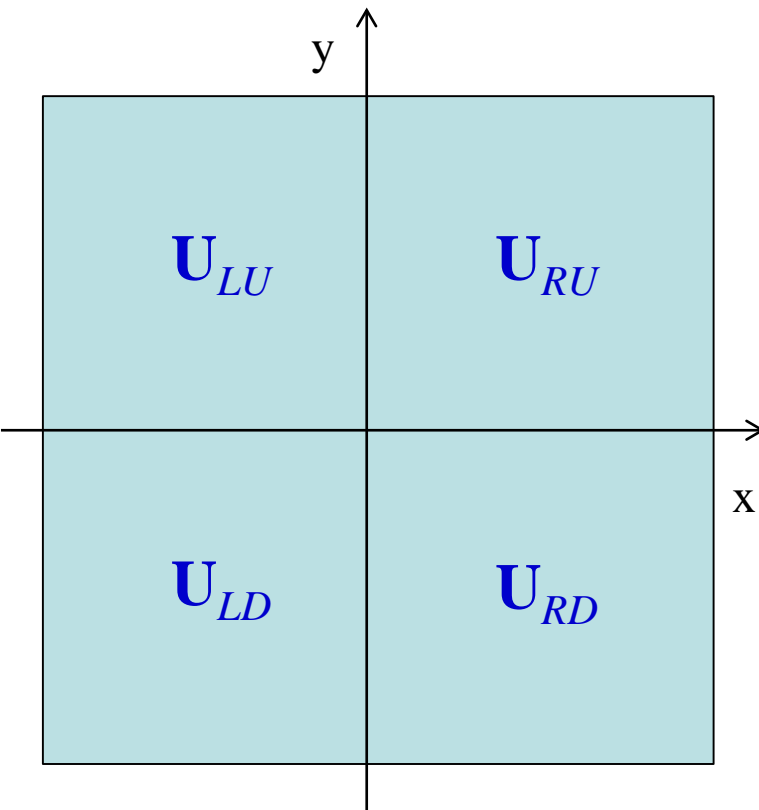
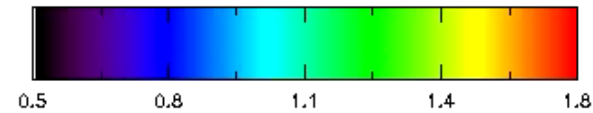
The introduction of the **subsonic constant state U^*** , whether in 1D or 2D, provides the requisite **dissipation** as well as **entropy enforcement**.



IV) Formulating the Multid. Riemann Solver in Similarity Variables

Two-Dimensional Riemann Problems have been explored (using 1D RS technology) by Shulz-Rinne et al (1993).

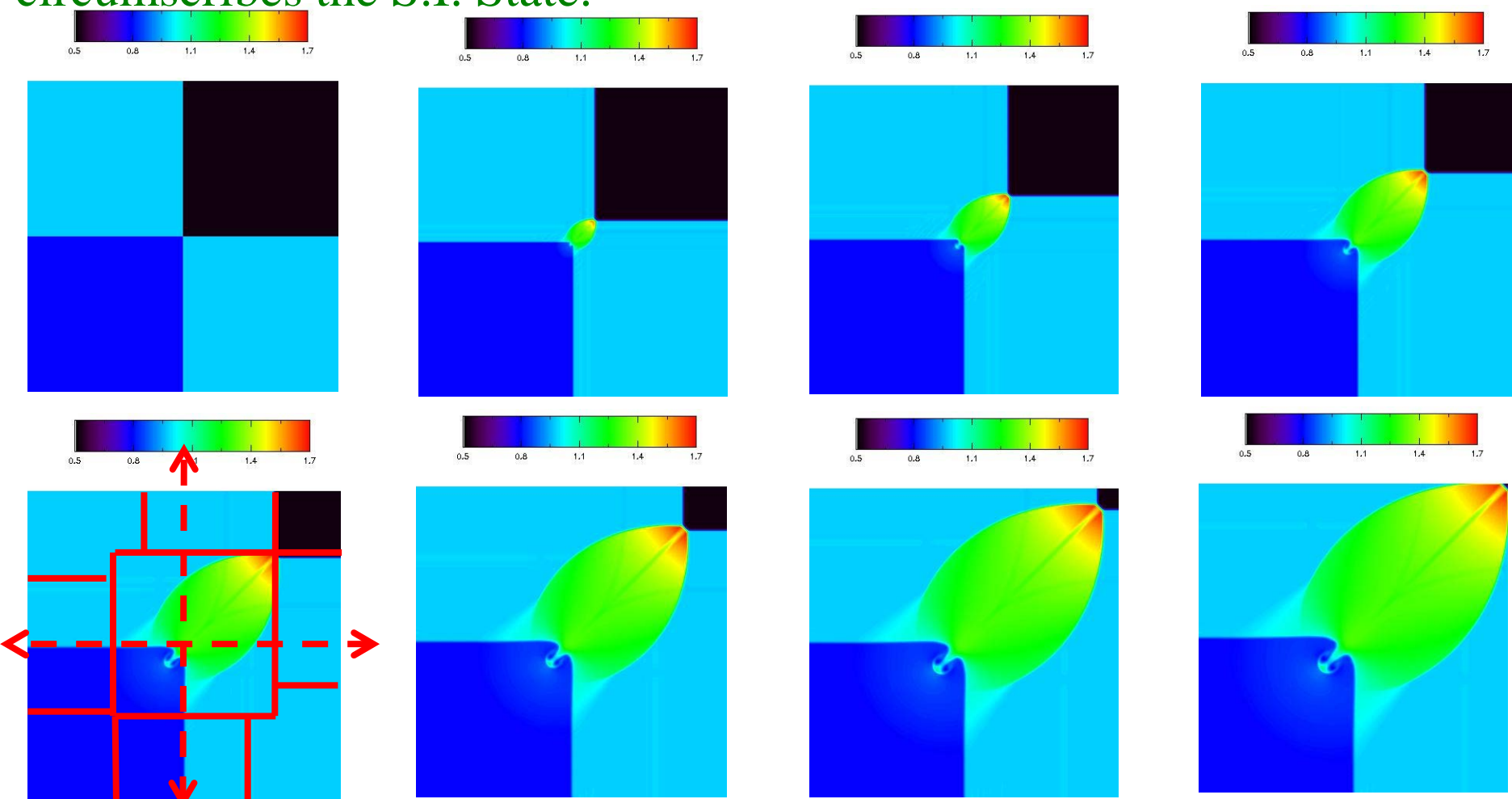
They arise when **four constant states** come together **at a corner**. See the **four** states U_{RU} , U_{LU} , U_{LD} and U_{RD} and their evolution in time-sequence:



The Strongly-Interacting State (**S.I.State**) is formed by the **interaction of four 1D Riemann problems**. Notice the Self-Similarity of S.I. State!

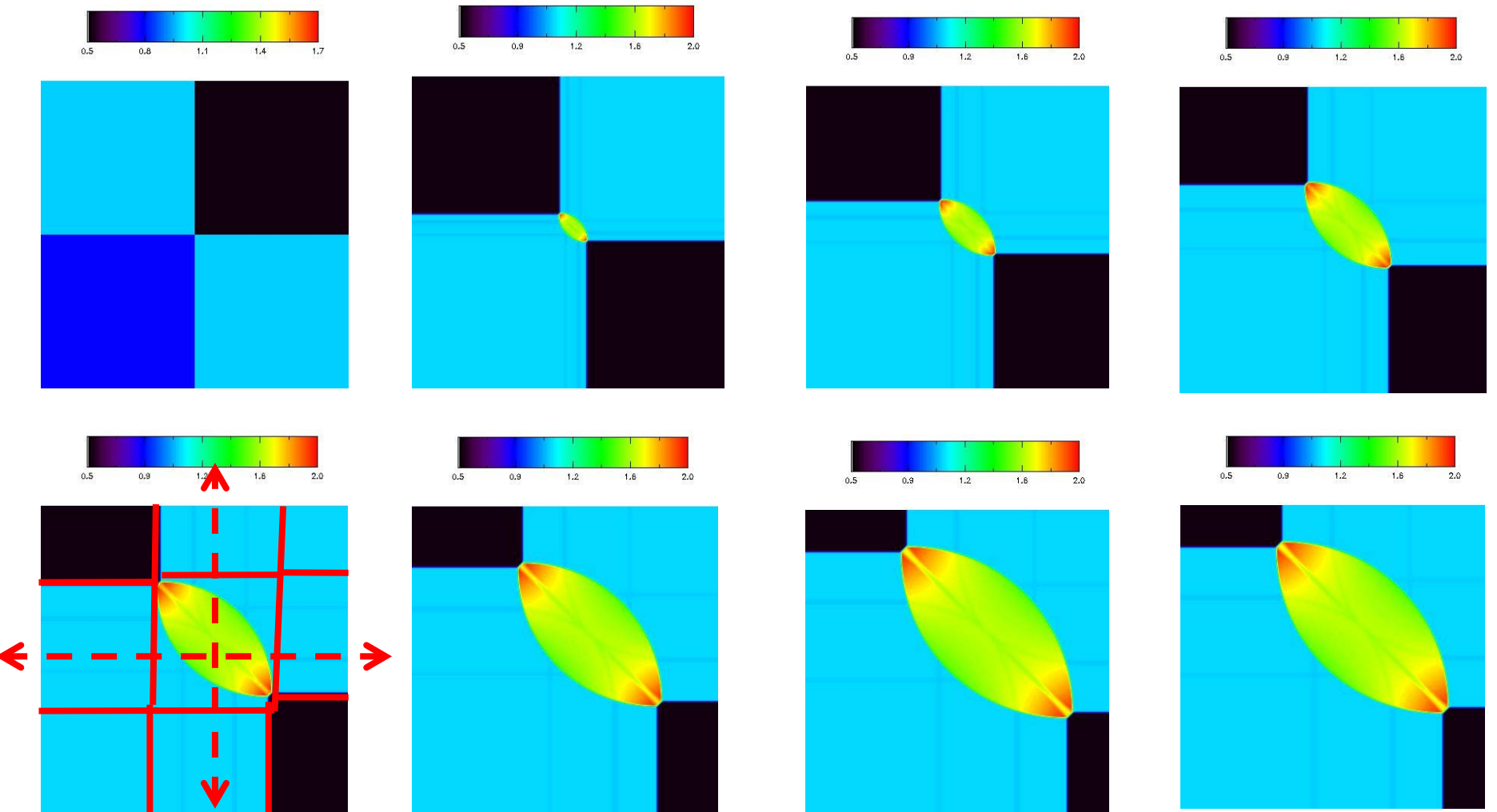
The S.I. State is bounded by the four 1D Riemann problems. This gives us the **Wave Model**. 1D RPs help us pick out multid. Wave model!

The 1D RP's lie within the boundaries of the Wave Model which circumscribes the S.I. State.



Notice the Self-Similarity of the Strongly-Interacting State!

Observe that as the strongly-interacting state moves outward, it engulfs the one-dimensional Riemann problems! Importance of **Lagrangian flux**! In that sense, the one-dimensional Riemann problems literally provide the boundary conditions for the multidimensional Riemann problem.



Game Plan:

- 1) Use 1D RPs to identify the boundaries of the **Multidimensional Wave Model**.
- 2) Assert **self-similar evolution of the Strongly Interacting State** within the Multidimensional Wave Model.
- 3) Recast the **Conservation Law in similarity variables**.
- 4) **Solve for the Strongly Interacting State** using 1D RP as boundary conditions for the Multidimensional Wave Model.

The Result:

**MuSIC RS == Multidimensional, Self-similar, strongly-
Interacting, Consistent Riemann Solver**

Use similarity variables!

Consider $\frac{\partial \mathbf{U}(x,t)}{\partial t} + \frac{\partial \mathbf{F}(x,t)}{\partial x} = 0$ and replace *two* coordinates, (x,t) ,

with *one* similarity variable $\xi = \frac{x}{t}$

$$\frac{\partial \mathbf{U}}{\partial t} =$$

$$\frac{\partial \mathbf{F}}{\partial x} =$$

$$\frac{\partial \mathbf{U}}{\partial t} + \frac{\partial \mathbf{F}}{\partial x} =$$

Consider $\frac{\partial \mathbf{U}(x,t)}{\partial t} + \frac{\partial \mathbf{F}(x,t)}{\partial x} = 0$ and replace *two* coordinates, (x,t) ,

with *one* similarity variable $\xi = \frac{x}{t}$

$$\frac{\partial \mathbf{U}}{\partial t} = \frac{\partial \xi}{\partial t} \frac{\partial \mathbf{U}}{\partial \xi} = -\frac{x}{t^2} \frac{\partial \mathbf{U}}{\partial \xi} = -\frac{1}{t} \xi \frac{\partial \mathbf{U}}{\partial \xi}$$

$$\frac{\partial \mathbf{F}}{\partial x} = \frac{\partial \xi}{\partial x} \frac{\partial \mathbf{F}}{\partial \xi} = \frac{1}{t} \frac{\partial \mathbf{F}}{\partial \xi}$$

$$\frac{\partial \mathbf{U}}{\partial t} + \frac{\partial \mathbf{F}}{\partial x} = -\frac{1}{t} \xi \frac{\partial \mathbf{U}}{\partial \xi} + \frac{1}{t} \frac{\partial \mathbf{F}}{\partial \xi} = 0$$

$$\Leftrightarrow \frac{\partial \mathbf{F}}{\partial \xi} - \xi \frac{\partial \mathbf{U}}{\partial \xi} = 0 \quad \Leftrightarrow \frac{\partial (\mathbf{F} - \xi \mathbf{U})}{\partial \xi} + \mathbf{U} = 0$$

How to Work With Similarity Variables in Multidimensions?

Insert $\tilde{\xi} = \frac{x}{t}$; $\tilde{\psi} = \frac{y}{t}$ in $\frac{\partial \mathbf{U}}{\partial t} + \frac{\partial \mathbf{F}}{\partial x} + \frac{\partial \mathbf{G}}{\partial y} = 0$ Mnemonic: $x, y \rightarrow ksi, psi$

In Similarity variables:-

Replace *three* coordinates (x, y, t) with *two* similarity variables $(\tilde{\xi}, \tilde{\psi})$:-

$$\mathbf{U}(x, y, t) \rightarrow \tilde{\mathbf{U}}(\tilde{\xi}, \tilde{\psi}) ; \mathbf{F}(x, y, t) \rightarrow \tilde{\mathbf{F}}(\tilde{\xi}, \tilde{\psi}) ; \mathbf{G}(x, y, t) \rightarrow \tilde{\mathbf{G}}(\tilde{\xi}, \tilde{\psi})$$

We Get:
$$\frac{\partial(\tilde{\mathbf{F}} - \tilde{\xi}\tilde{\mathbf{U}})}{\partial \tilde{\xi}} + \frac{\partial(\tilde{\mathbf{G}} - \tilde{\psi}\tilde{\mathbf{U}})}{\partial \tilde{\psi}} + 2\tilde{\mathbf{U}} = 0$$

With a slight shift and rescaling of variables, we get:

$$\frac{1}{\Delta \xi} \frac{\partial [\tilde{\mathbf{F}} - (\xi_c + \xi \Delta \xi) \tilde{\mathbf{U}}]}{\partial \xi} + \frac{1}{\Delta \psi} \frac{\partial [\tilde{\mathbf{G}} - (\psi_c + \psi \Delta \psi) \tilde{\mathbf{U}}]}{\partial \psi} + 2\tilde{\mathbf{U}} = 0$$

This is the Master Equation!

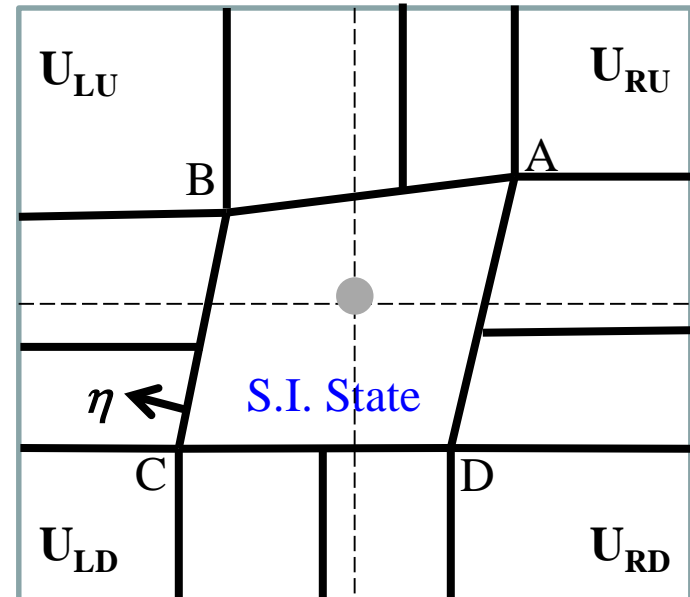
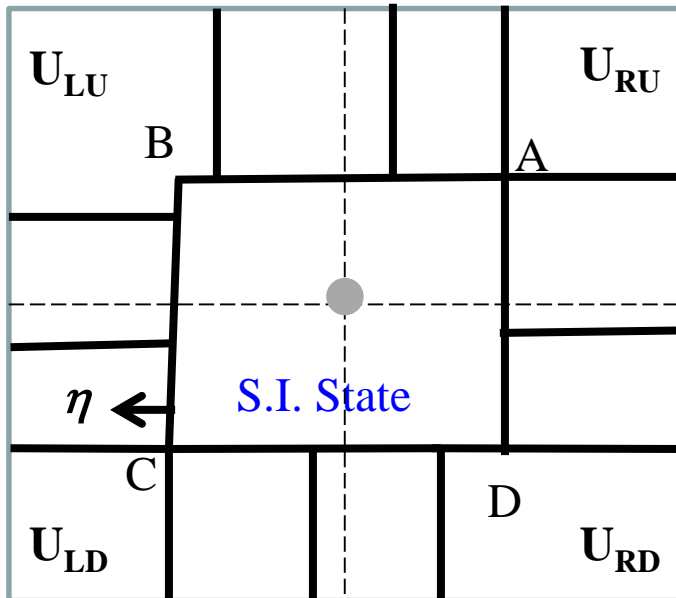
Solution methodology: Assert **Self-Similar** solution using **self-similar trial/basis** functions:

$$\tilde{U}(\xi, \psi) = \bar{U} + \mathbf{U}_\xi \xi + \mathbf{U}_\psi \psi + \mathbf{U}_{\xi\xi} \left[\xi^2 - \frac{1}{12} \right] + \mathbf{U}_{\psi\psi} \left[\psi^2 - \frac{1}{12} \right] + \mathbf{U}_{\xi\psi} \xi \psi \quad (\text{Similarly for fluxes!})$$



Using **test functions** $\phi(\xi, \psi)$, in **Galerkin sense**, integrate Master Equation over S.I. State:

$$\frac{1}{\Delta\xi} \frac{\partial \left\{ \phi(\xi, \psi) \left[\tilde{\mathbf{F}} - (\xi_c + \xi \Delta\xi) \tilde{\mathbf{U}} \right] \right\}}{\partial \xi} + \frac{1}{\Delta\psi} \frac{\partial \left\{ \phi(\xi, \psi) \left[\tilde{\mathbf{G}} - (\psi_c + \psi \Delta\psi) \tilde{\mathbf{U}} \right] \right\}}{\partial \psi} - \frac{1}{\Delta\xi} \left[\tilde{\mathbf{F}} - (\xi_c + \xi \Delta\xi) \tilde{\mathbf{U}} \right] \frac{\partial \phi(\xi, \psi)}{\partial \xi} - \frac{1}{\Delta\psi} \left[\tilde{\mathbf{G}} - (\psi_c + \psi \Delta\psi) \tilde{\mathbf{U}} \right] \frac{\partial \phi(\xi, \psi)}{\partial \psi} + 2 \phi(\xi, \psi) \tilde{\mathbf{U}} = 0$$



If there is no sub-structure (i.e., $\tilde{U}(\xi, \psi) = \bar{U}$ etc.) we get **3 V.Imp. Eqns.:**

$$2 A_{ABCD} \bar{U} = -\frac{1}{\Delta S} \int_{A \rightarrow B \rightarrow C \rightarrow D \rightarrow A} (\mathbf{F}_\eta(\ell) - S_\eta \mathbf{U}(\ell)) d\ell \leftarrow \text{Gives State}$$

$$-\frac{A_{ABCD}}{\Delta S} \bar{\mathbf{F}} = -\frac{\xi_c}{\Delta S} A_{ABCD} \bar{U} - \frac{1}{\Delta S} \int_{A \rightarrow B \rightarrow C \rightarrow D \rightarrow A} \xi (\mathbf{F}_\eta(\ell) - S_\eta \mathbf{U}(\ell)) d\ell$$

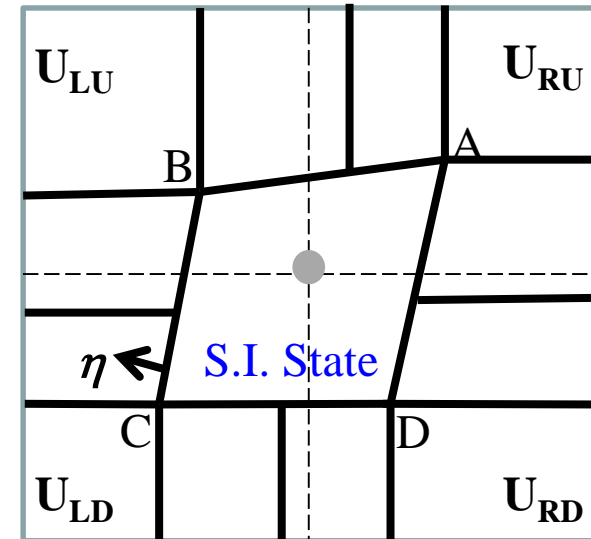
$$-\frac{A_{ABCD}}{\Delta S} \bar{\mathbf{G}} = -\frac{\psi_c}{\Delta S} A_{ABCD} \bar{U} - \frac{1}{\Delta S} \int_{A \rightarrow B \rightarrow C \rightarrow D \rightarrow A} \psi (\mathbf{F}_\eta(\ell) - S_\eta \mathbf{U}(\ell)) d\ell$$

\leftarrow Gives x- and y-fluxes

Use **Gauss Law**, Integrate over S.I. State

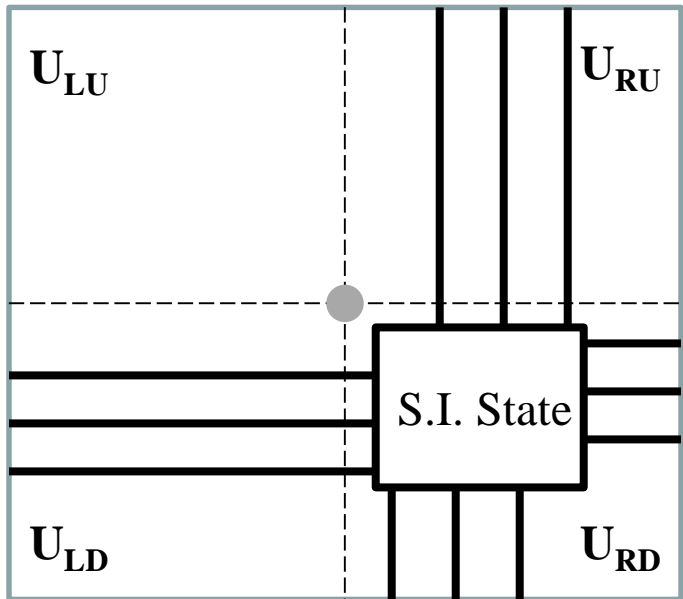
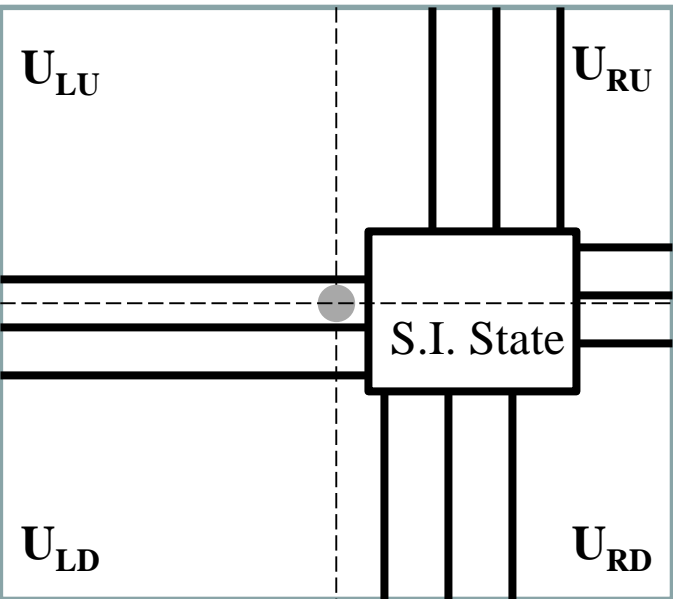
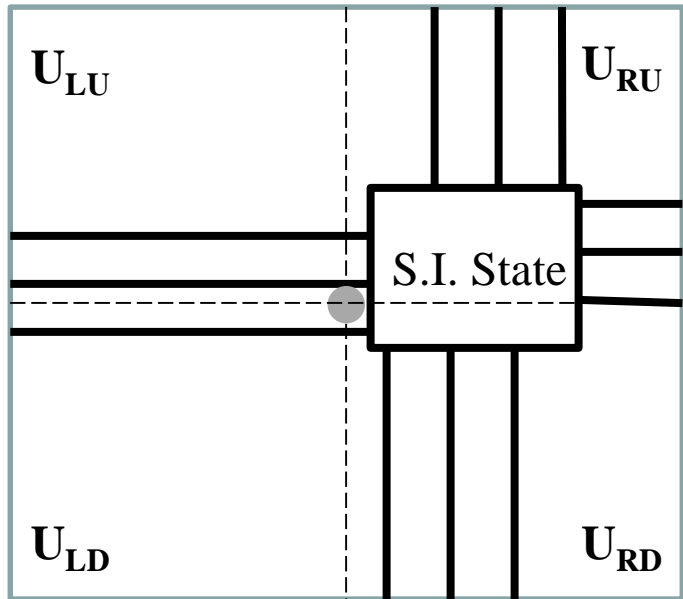
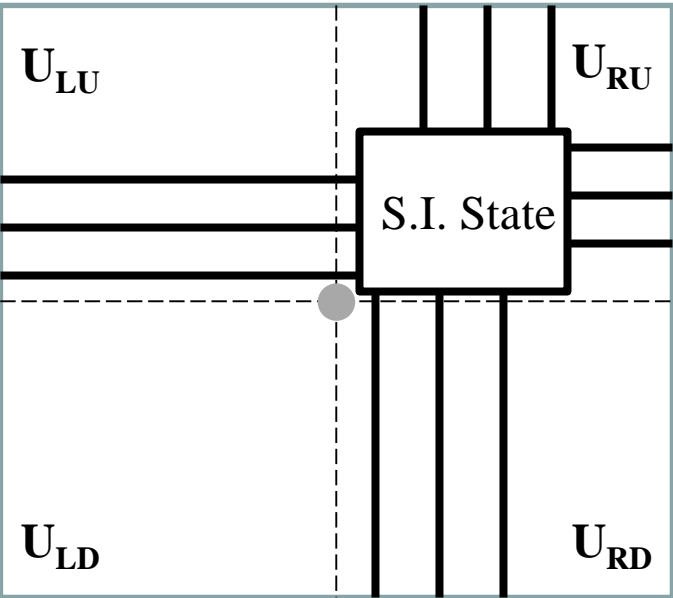
Interpret above equations physically – they depend on **Lagrangian flux**! Reason: The **Wave Model** is a **moving boundary**! **Multid. Wave model eats into 1d RP!**

State and fluxes are **uniquely defined** by values in the 1D Riemann problems that lie in the boundary of the S.I. State.



These **Integral Constraints** **MUST** be respected!

Supersonic cases are easily treated, Illustrated here for the 1D HLLC RS when flow is supersonic to the right. S.I. State does not overlie vertex.



Introducing **Sub-Structure in the Strongly-Interacting State** is easy – Just retain more moments and the Galerkin formulation does the rest!

Start with: $\tilde{\mathbf{U}}(\xi, \psi) = \bar{\mathbf{U}} + \mathbf{U}_\xi \xi + \mathbf{U}_\psi \psi$; $\tilde{\mathbf{F}}(\xi, \psi) = \bar{\mathbf{F}} + \mathbf{F}_\xi \xi + \mathbf{F}_\psi \psi$; $\tilde{\mathbf{G}}(\xi, \psi) = \bar{\mathbf{G}} + \mathbf{G}_\xi \xi + \mathbf{G}_\psi \psi$

For example, **Integrating the test function $\phi(\xi, \psi) = \xi$ over the wave model**, we get:

$$\frac{1}{4} \mathbf{U}_\xi - \frac{1}{\Delta \xi} \bar{\mathbf{F}} = -\frac{\xi_c}{\Delta \xi} \bar{\mathbf{U}}$$

$$- \left[\frac{1}{2\Delta \xi} \int_{-1/2}^{1/2} (\mathbf{F}(1/2, \psi) - S_R \mathbf{U}(1/2, \psi)) d\psi + \frac{1}{2\Delta \xi} \int_{-1/2}^{1/2} (\mathbf{F}(-1/2, \psi) - S_L \mathbf{U}(-1/2, \psi)) d\psi \right]$$

$$+ \frac{1}{\Delta \psi} \int_{-1/2}^{1/2} \xi (\mathbf{G}(\xi, 1/2) - S_U \mathbf{U}(\xi, 1/2)) d\xi - \frac{1}{\Delta \psi} \int_{-1/2}^{1/2} \xi (\mathbf{G}(\xi, -1/2) - S_D \mathbf{U}(\xi, -1/2)) d\xi$$

For example, **Integrating the test function $\phi(\xi, \psi) = \psi$ over the wave model**, we get:

$$\frac{1}{4} \mathbf{U}_\psi - \frac{1}{\Delta \psi} \bar{\mathbf{G}} = -\frac{\psi_c}{\Delta \psi} \bar{\mathbf{U}}$$

$$- \left[\frac{1}{\Delta \xi} \int_{-1/2}^{1/2} \psi (\mathbf{F}(1/2, \psi) - S_R \mathbf{U}(1/2, \psi)) d\psi - \frac{1}{\Delta \xi} \int_{-1/2}^{1/2} \psi (\mathbf{F}(-1/2, \psi) - S_L \mathbf{U}(-1/2, \psi)) d\psi \right]$$

$$+ \frac{1}{2\Delta \psi} \int_{-1/2}^{1/2} (\mathbf{G}(\xi, 1/2) - S_U \mathbf{U}(\xi, 1/2)) d\xi + \frac{1}{2\Delta \psi} \int_{-1/2}^{1/2} (\mathbf{G}(\xi, -1/2) - S_D \mathbf{U}(\xi, -1/2)) d\xi$$

Further equations detailed in papers.

This process has been explicitly carried out for **linear** variations in Balsara (2014), Balsara & Dumbser (2015), Balsara *et al.* (2016a,b).

Methods to treat linearly degenerate waves (which need to have their profiles steepened) and genuinely nonlinear waves (which do not need steepening) are also documented in these papers.

V) Approximating the Multidimensional Riemann Problem with just ONE call to the Multidimensional Riemann Solver!

$$\tilde{\mathbf{U}}(\xi, \psi) = \bar{\mathbf{U}} + \mathbf{U}_\xi \xi + \mathbf{U}_\psi \psi + \mathbf{U}_{\xi\xi} \left[\xi^2 - \frac{1}{12} \right] + \mathbf{U}_{\psi\psi} \left[\psi^2 - \frac{1}{12} \right] + \mathbf{U}_{\xi\psi} \xi \psi \quad ;$$

Linearize fluxes: (using $\bar{\mathbf{A}} \equiv \partial \bar{\mathbf{F}}(\bar{\mathbf{U}}) / \partial \bar{\mathbf{U}}$ and $\bar{\mathbf{B}} \equiv \partial \bar{\mathbf{G}}(\bar{\mathbf{U}}) / \partial \bar{\mathbf{U}}$)

$$\tilde{\mathbf{F}}(\xi, \psi) = \bar{\mathbf{F}}(\bar{\mathbf{U}}) + \bar{\mathbf{A}} (\tilde{\mathbf{U}}(\xi, \psi) - \bar{\mathbf{U}}) \quad ; \quad \tilde{\mathbf{G}}(\xi, \psi) = \bar{\mathbf{G}}(\bar{\mathbf{U}}) + \bar{\mathbf{B}} (\tilde{\mathbf{U}}(\xi, \psi) - \bar{\mathbf{U}})$$

$$2\bar{\mathbf{U}} = - \left[\begin{aligned} & \frac{1}{\Delta\xi} \int_{-1/2}^{1/2} (\mathbf{F}(1/2, \psi) - S_R \mathbf{U}(1/2, \psi)) d\psi - \frac{1}{\Delta\xi} \int_{-1/2}^{1/2} (\mathbf{F}(-1/2, \psi) - S_L \mathbf{U}(-1/2, \psi)) d\psi \\ & + \frac{1}{\Delta\psi} \int_{-1/2}^{1/2} (\mathbf{G}(\xi, 1/2) - S_U \mathbf{U}(\xi, 1/2)) d\xi - \frac{1}{\Delta\psi} \int_{-1/2}^{1/2} (\mathbf{G}(\xi, -1/2) - S_D \mathbf{U}(\xi, -1/2)) d\xi \end{aligned} \right]$$

$$\frac{1}{4} \mathbf{U}_\xi = \frac{1}{\Delta\xi} (\bar{\mathbf{F}} - \xi_c \bar{\mathbf{U}})$$

$$- \left[\begin{aligned} & \frac{1}{2\Delta\xi} \int_{-1/2}^{1/2} (\mathbf{F}(1/2, \psi) - S_R \mathbf{U}(1/2, \psi)) d\psi + \frac{1}{2\Delta\xi} \int_{-1/2}^{1/2} (\mathbf{F}(-1/2, \psi) - S_L \mathbf{U}(-1/2, \psi)) d\psi \\ & + \frac{1}{\Delta\psi} \int_{-1/2}^{1/2} \xi (\mathbf{G}(\xi, 1/2) - S_U \mathbf{U}(\xi, 1/2)) d\xi - \frac{1}{\Delta\psi} \int_{-1/2}^{1/2} \xi (\mathbf{G}(\xi, -1/2) - S_D \mathbf{U}(\xi, -1/2)) d\xi \end{aligned} \right]$$

$$\frac{1}{4} \mathbf{U}_\psi = \frac{1}{\Delta\psi} (\bar{\mathbf{G}} - \psi_c \bar{\mathbf{U}})$$

$$- \left[\frac{1}{\Delta\xi} \int_{-1/2}^{1/2} \psi (\mathbf{F}(1/2, \psi) - S_R \mathbf{U}(1/2, \psi)) d\psi - \frac{1}{\Delta\xi} \int_{-1/2}^{1/2} \psi (\mathbf{F}(-1/2, \psi) - S_L \mathbf{U}(-1/2, \psi)) d\psi \right]$$

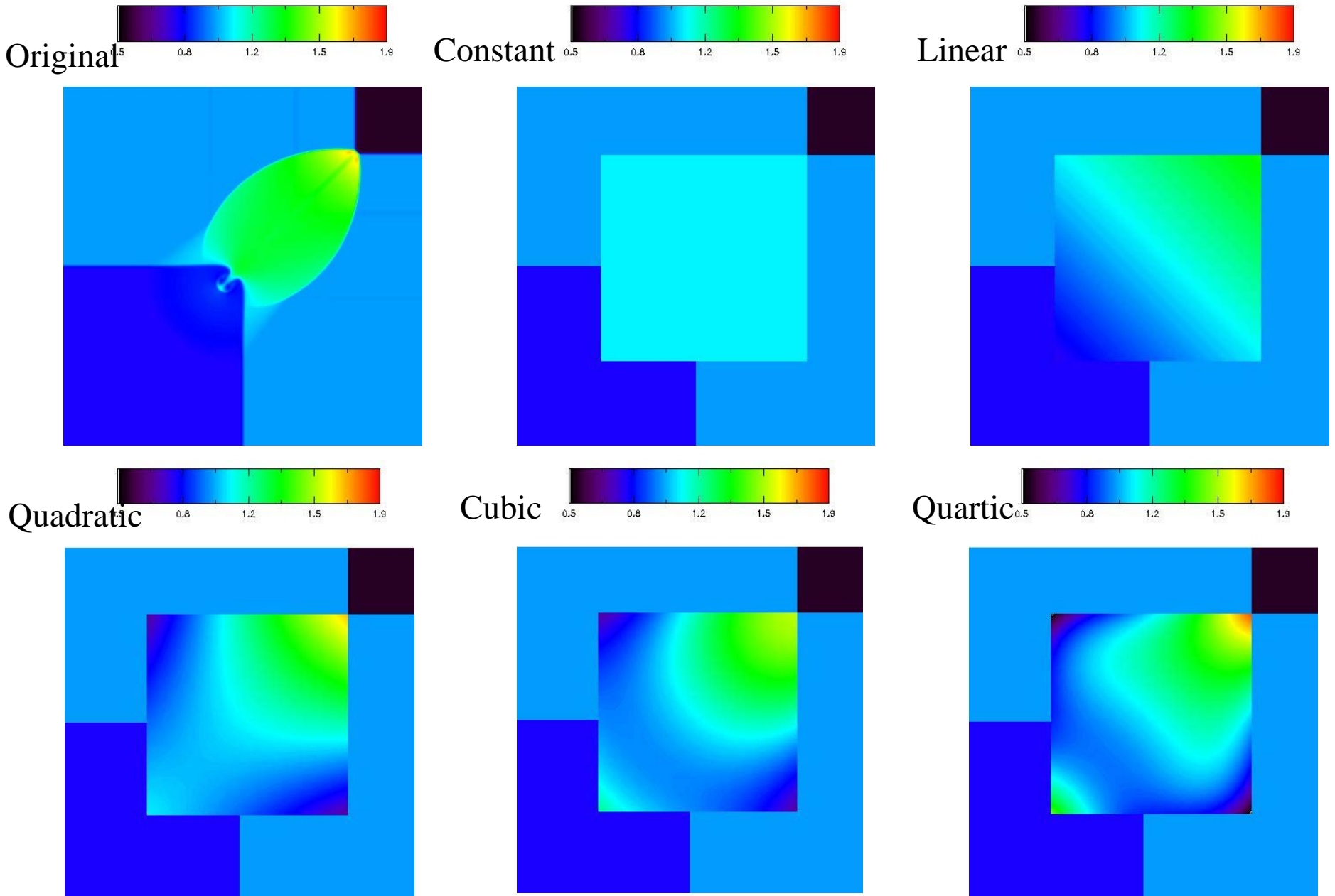
$$+ \frac{1}{2\Delta\psi} \int_{-1/2}^{1/2} (\mathbf{G}(\xi, 1/2) - S_U \mathbf{U}(\xi, 1/2)) d\xi + \frac{1}{2\Delta\psi} \int_{-1/2}^{1/2} (\mathbf{G}(\xi, -1/2) - S_D \mathbf{U}(\xi, -1/2)) d\xi$$

Further equations detailed in paper.

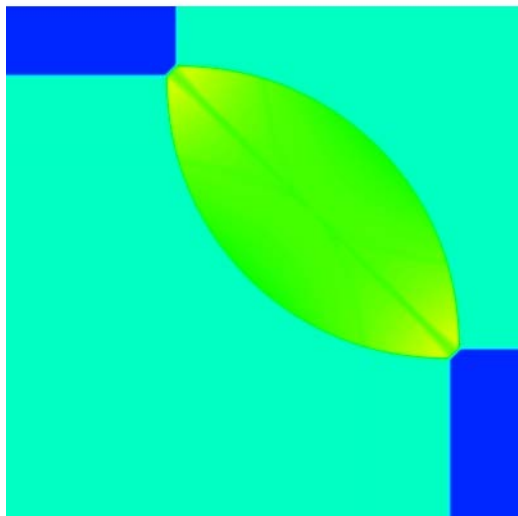
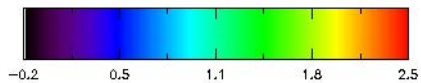
While this process has been demonstrated for **linear** variations, **quadratic**, **cubic** and **quartic** variations have also been documented in Balsara (2014).

Allows us to construct a series solution for the multidimensional Riemann problem.

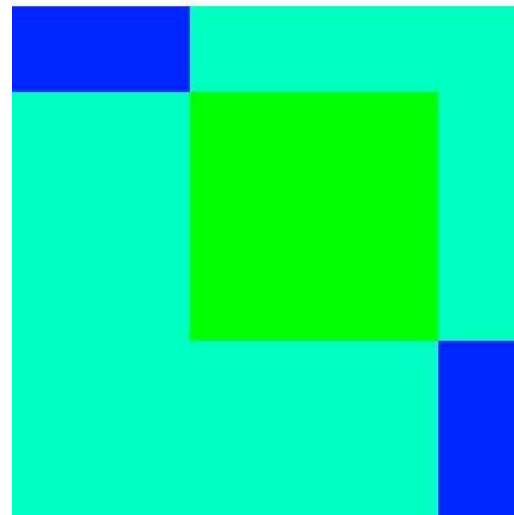
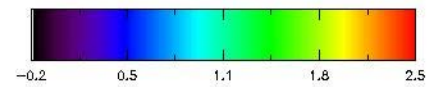
V) Approximating the Multidimensional Riemann Problem with just ONE call to the Multidimensional Riemann Solver!



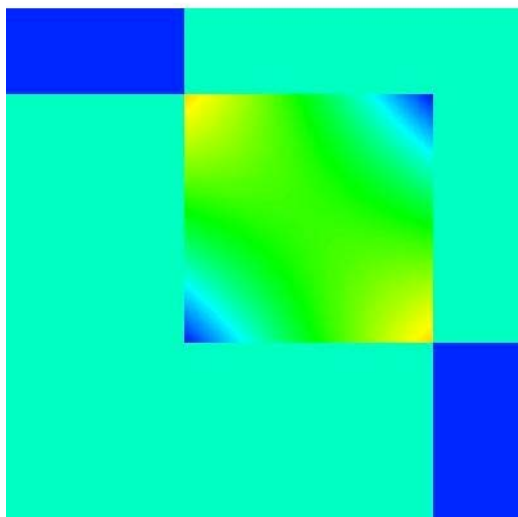
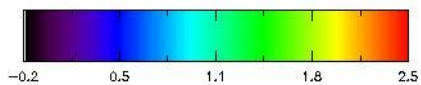
Original



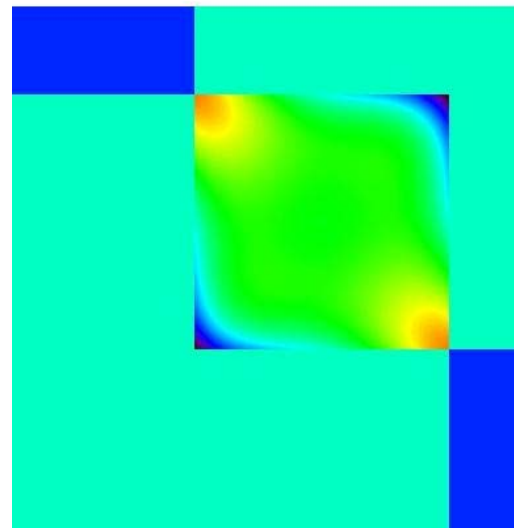
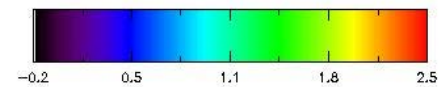
Constant



Quadratic



Quartic



VI) Results & Applications

Accuracy analysis for multi-d RS presented in Balsara (2010, 2012, 2014, 2015) and Balsara, Dumbser & Abgrall (2014), Bosceri, Balsara & Dumbser (2014), Balsara & Dumbser (2015).

ADER is used in the predictor step with **WENO** reconstruction. **Multid. RS** provides the corrector step.

Test problems which emphasize **advantages of multi-d approach** are also presented. We find **vastly reduced mesh imprinting**.

CFL numbers that are higher than those in conventional 2nd order Godunov schemes are used.

Doubling dissipation for MHD is completely unnecessary.

Hydro, MHD & RMHD tests presented.

ANY self-similar 1D Riemann solver can be used in the Multid RS! ⁴⁸

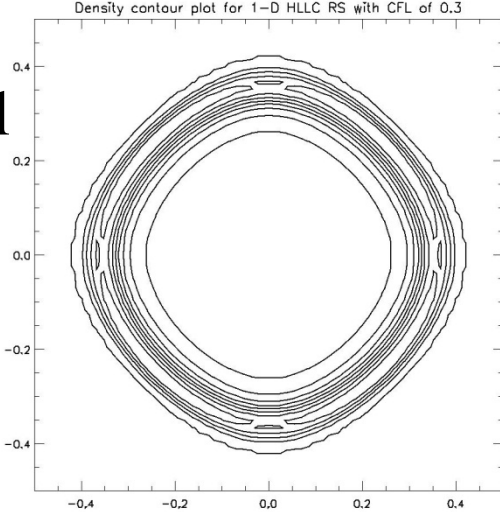
Euler Flow: Spherical 3D Hydrodynamical Blast problem.

With sufficient resolution, all test problems will pin this one well.

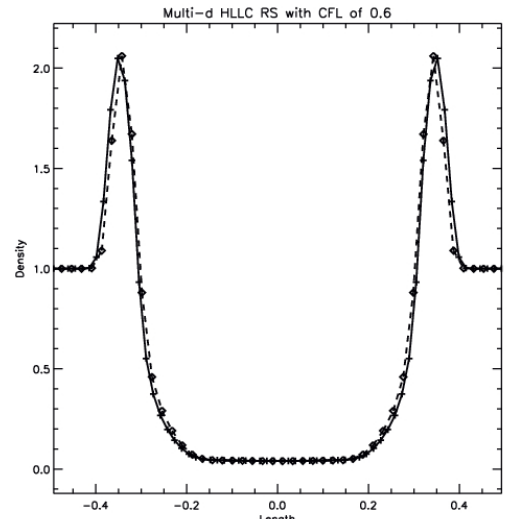
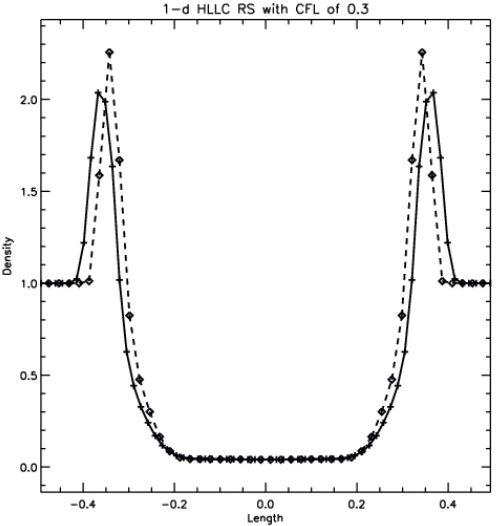
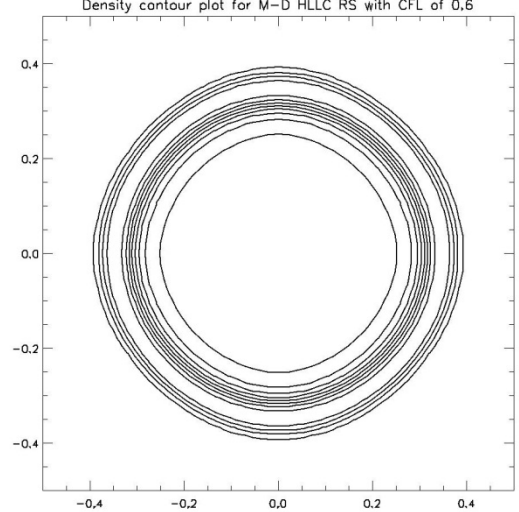
However, real applications are resolution-starved. 64^3 zones in 3D.

On coarser meshes, mesh imprinting shows up; latter is more **isotropic**.

Conventional
2nd order:
(CFL 0.3)



With 2D
HLLC RS:
(CFL 0.6)



Euler Flow: Isentropic Vortex – Accuracy Analysis on Unstructured Mesh

Run with CFL of 0.95. Accuracy shown with increasing mesh resolution. ADER-WENO Schemes used.

Second order:

#of elements, 1d	L ₁ Error	L ₁ Order	L ₂ Error	L ₂ Order	L _∞ Error	L _∞ Order
64	2.2707E-01		3.7415E-02		2.4855E-02	
128	5.1411E-02	2.14	8.1563E-03	2.20	6.7079E-03	1.89
256	1.3657E-02	1.91	2.1622E-03	1.92	1.8540E-03	1.86
512	3.5597E-03	1.94	5.7674E-04	1.91	4.4355E-04	2.06

Third order:

#of elements, 1d	L ₁ Error	L ₁ Order	L ₂ Error	L ₂ Order	L _∞ Error	L _∞ Order
64	7.0733E-02		1.7641E-02		1.0994E-02	
128	9.9983E-03	2.82	2.5492E-03	2.79	1.5428E-03	2.83
256	1.2705E-03	2.98	3.2764E-04	2.96	1.9774E-04	2.96
512	1.5977E-04	2.99	4.1369E-05	2.99	2.5654E-05	2.95

Fourth order:

#of elements, 1d	L ₁ Error	L ₁ Order	L ₂ Error	L ₂ Order	L _∞ Error	L _∞ Order
64	9.1699E-03		1.8107E-03		1.2780E-03	
128	4.6866E-04	4.29	9.3267E-05	4.28	8.7567E-05	3.87
256	2.8738E-05	4.03	5.7309E-06	4.02	5.8208E-06	3.91
512	1.7730E-06	4.02	3.5168E-07	4.03	3.5236E-07	4.05

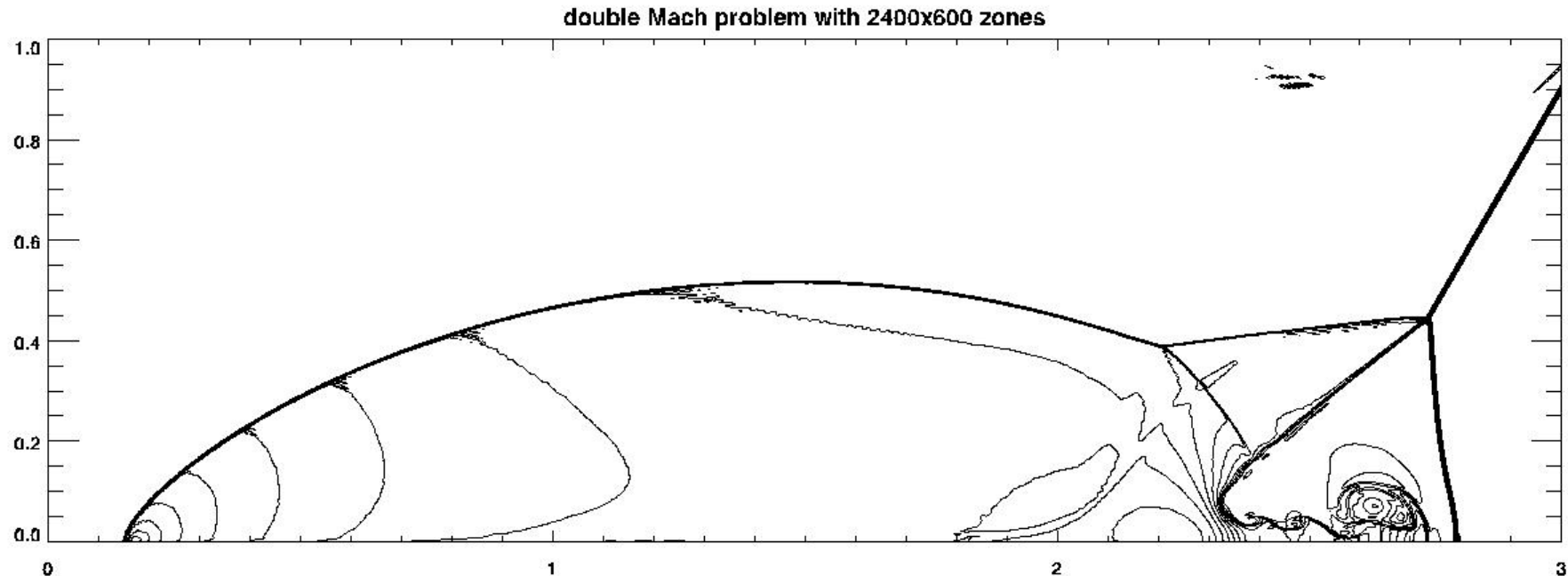
Euler Flow: Double Mach Reflection Problem on Structured Mesh

Run with CFL of 0.8. Usually requires a 1920x480 zone mesh to see the KH instability at the Mach stem even with 4th order DG methods.

Results at 2400x600 zones with 2nd order shown here

Multid RS technology at 2nd order seems to catch up with high order schemes with conventional RS technology.

CFL # vastly larger than that for 4th order DG schemes!



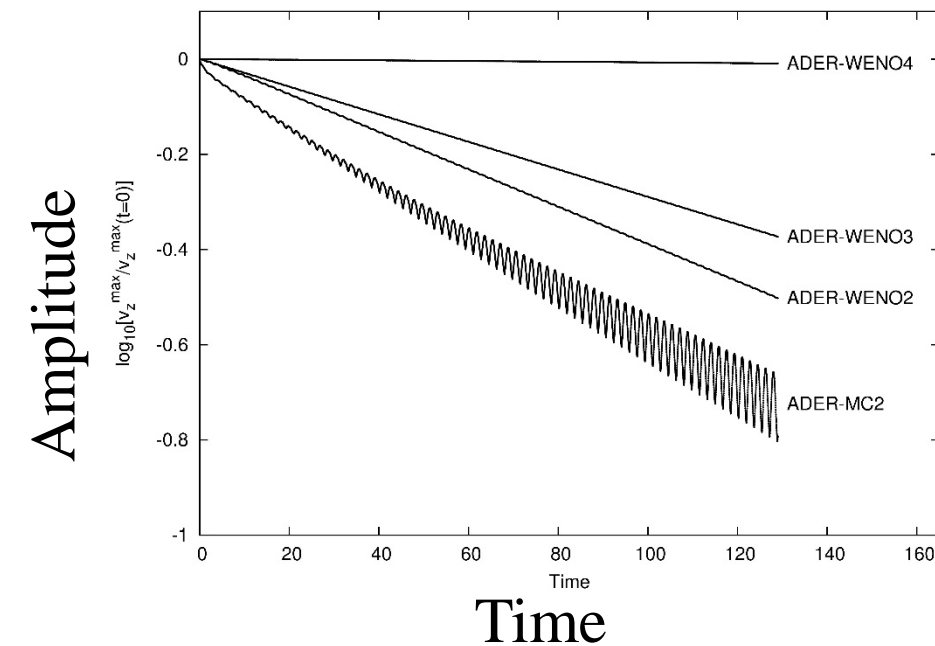
MHD Flow: Long term decay of Alfvén Waves

Alfvén waves propagating very obliquely to mesh.

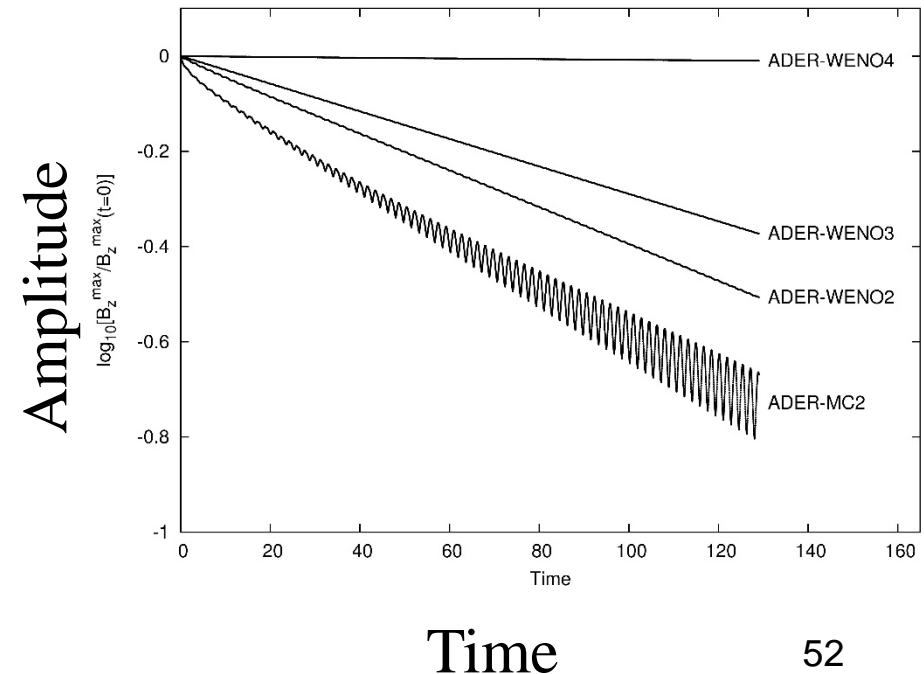
The decay over long times is shown. Of all the choices shown, **2D HLLD RS** with some amount of WENO technology shows the least dissipation.

Effect of **second, third and fourth order of accuracy** also shown.

Decay of V_z



Decay of B_z



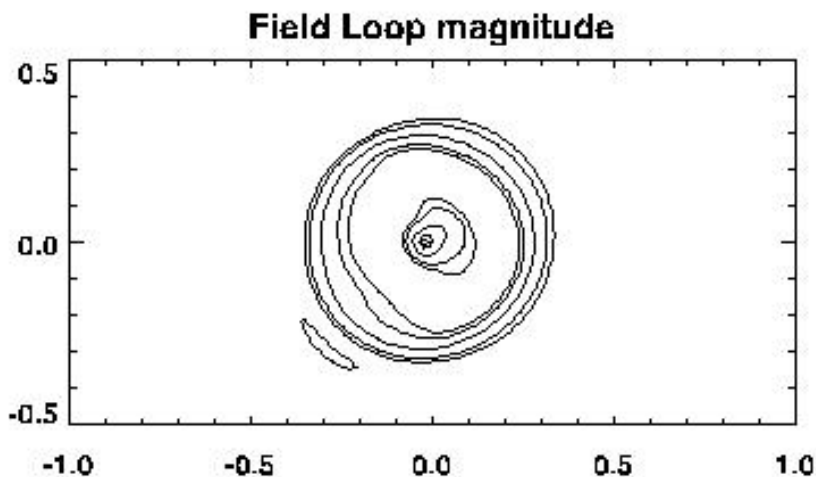
MHD Flow: Magnetic Field Loop Advection

Run with CFL of 0.9. Magnetic loop advected diagonally on a rectangular domain.

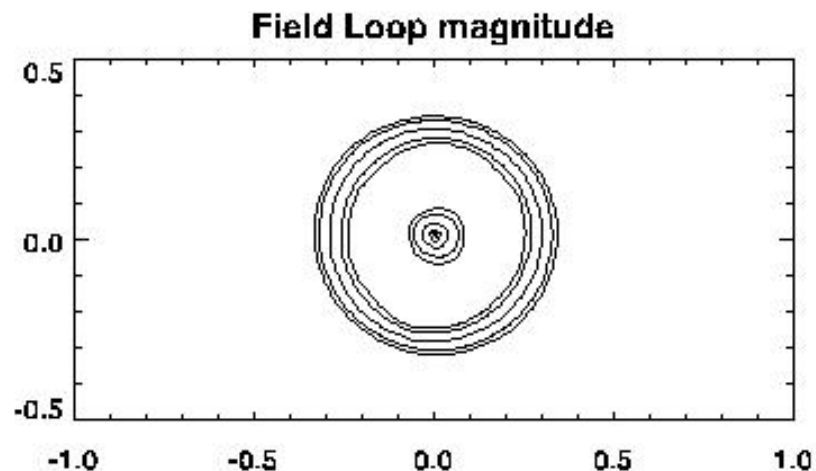
Conventional scheme doubles dissipation of the electric field (Gardiner & Stone 2005). The scheme with Multid. RS does not double dissipation.

The propagation of the field loop is much **more isotropic for Multid. RS**

Conventional 2nd order
(Gardiner & Stone 2005):
(CFL 0.45)

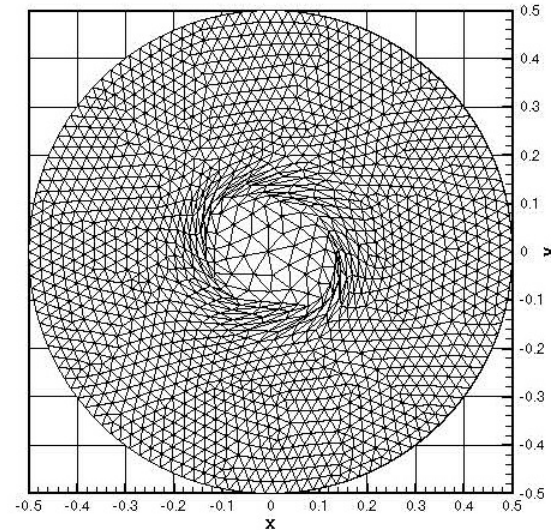
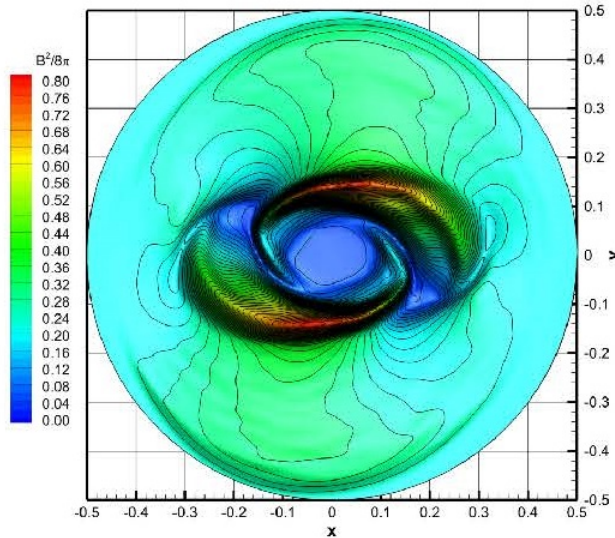
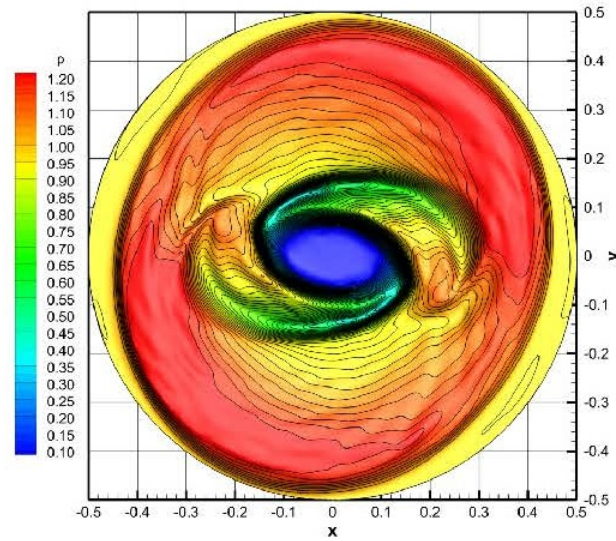
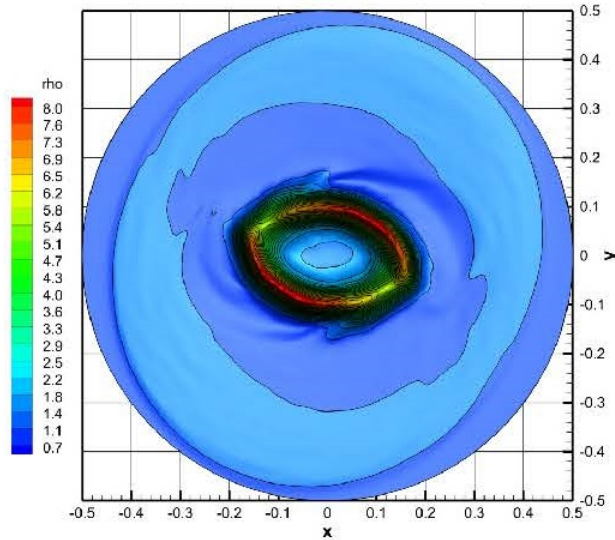


With 2D HLLC RS
Balsara (2010, 2012):
(CFL 0.9)



MHD Rotor Problem on ALE Mesh

CFL 0.9; 80,000 elements ; ALE mesh



Accuracy for the MHD Vortex problem on an ALE Mesh

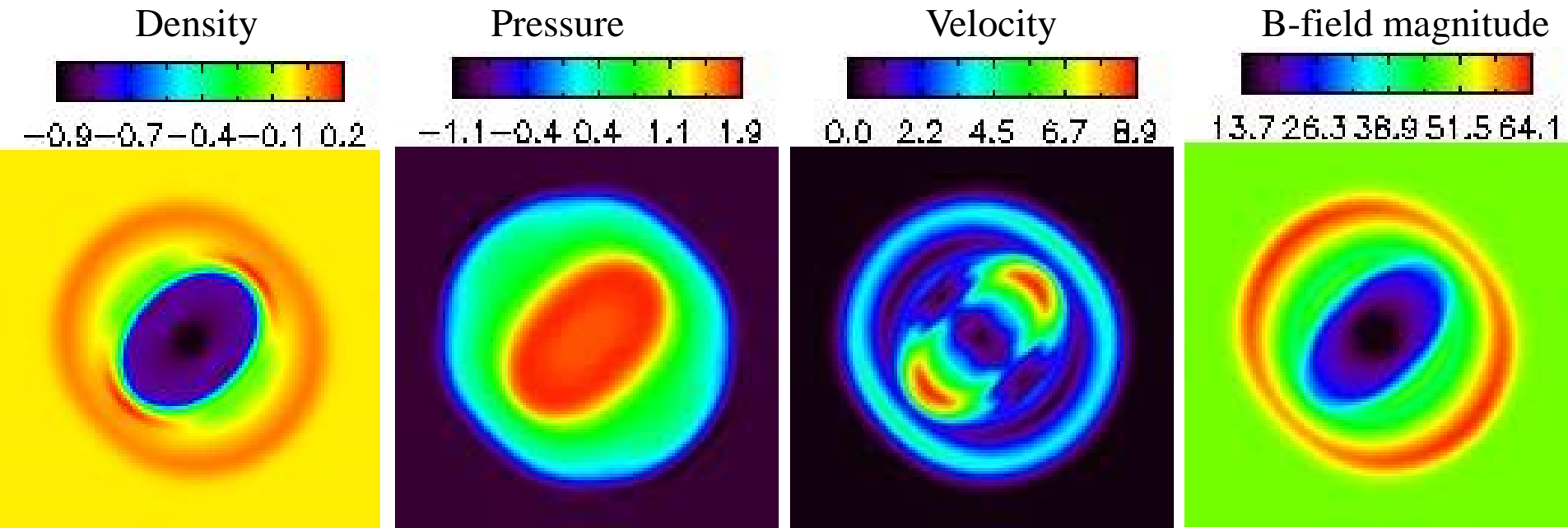
Accuracy demonstrated from 1st to 5th order on 2D ALE Mesh.

	$h(\Omega(t_f))$	\mathcal{NS}_{cs} ϵ_{L_2}	$\mathcal{O}(L_2)$	$h(\Omega, t_f)$	\mathcal{NS}_m ϵ_{L_2}	$\mathcal{O}(L_2)$	$h(\Omega, t_f)$	\mathcal{NS}_b ϵ_{L_2}	$\mathcal{O}(L_2)$
					$\mathcal{O}1$				
	3.26E-01	2.7330E-03	-	3.25E-01	2.7059E-03	-	3.26E-01	2.7381E-03	-
	2.37E-01	2.0111E-03	0.96	2.35E-01	2.0173E-03	0.90	2.35E-01	2.0173E-03	0.93
	1.64E-01	1.3081E-03	1.17	1.64E-01	1.3055E-03	1.20	1.64E-01	1.3113E-03	1.20
	1.28E-01	9.5497E-04	1.26	1.28E-01	9.5150E-04	1.30	1.28E-01	9.5617E-04	1.28
					$\mathcal{O}2$				
2 nd Order	3.26E-01	4.8091E-03	-	3.27E-01	4.7707E-03	-	3.26E-01	5.5971E-03	-
	2.35E-01	2.8382E-03	1.61	2.37E-01	2.8571E-03	1.58	2.35E-01	2.7874E-03	2.13
	1.64E-01	1.4212E-03	1.91	1.63E-01	1.4239E-03	1.88	1.63E-01	1.3789E-03	1.94
	1.28E-01	6.4686E-04	3.24	1.28E-01	6.4610E-04	3.26	1.28E-01	7.2141E-04	2.67
					$\mathcal{O}3$				
3 rd Order	3.25E-01	1.1417E-03	-	3.25E-01	1.1376E-03	-	3.26E-01	1.1265E-03	-
	2.36E-01	1.8935E-04	5.57	2.36E-01	1.8930E-04	5.56	2.36E-01	1.8632E-04	5.56
	1.63E-01	7.1734E-05	2.65	1.63E-01	7.1740E-05	2.65	1.63E-01	7.1912E-05	2.60
	1.28E-01	3.1651E-05	3.38	1.28E-01	3.1653E-05	3.38	1.28E-01	3.1738E-05	3.38
					$\mathcal{O}4$				
4 th Order	3.26E-01	2.4858E-04	-	3.26E-01	2.4864E-04	-	3.26E-01	2.4472E-04	-
	2.35E-01	7.9871E-05	3.50	2.35E-01	7.9875E-05	3.50	2.35E-01	7.9884E-05	3.45
	1.63E-01	2.1790E-05	3.55	1.63E-01	2.1791E-05	3.55	1.63E-01	2.1795E-05	3.55
	1.28E-01	8.2013E-06	4.03	1.28E-01	8.2014E-06	4.03	1.28E-01	8.1998E-06	4.03
					$\mathcal{O}5$				
5 th Order	3.26E-01	1.2010E-04	-	3.26E-01	1.2010E-04	-	3.26E-01	1.1992E-04	-
	2.35E-01	2.7365E-05	4.56	2.35E-01	2.7359E-05	4.56	2.35E-01	2.7327E-05	4.56
	1.63E-01	4.8779E-06	4.71	1.63E-01	4.8778E-06	4.71	1.63E-01	4.8898E-06	4.70
	1.28E-01	1.3947E-06	5.17	1.28E-01	1.3947E-06	5.17	1.28E-01	1.3935E-06	5.18

MHD Flow: 3D MHD Blast with very low Plasma Beta

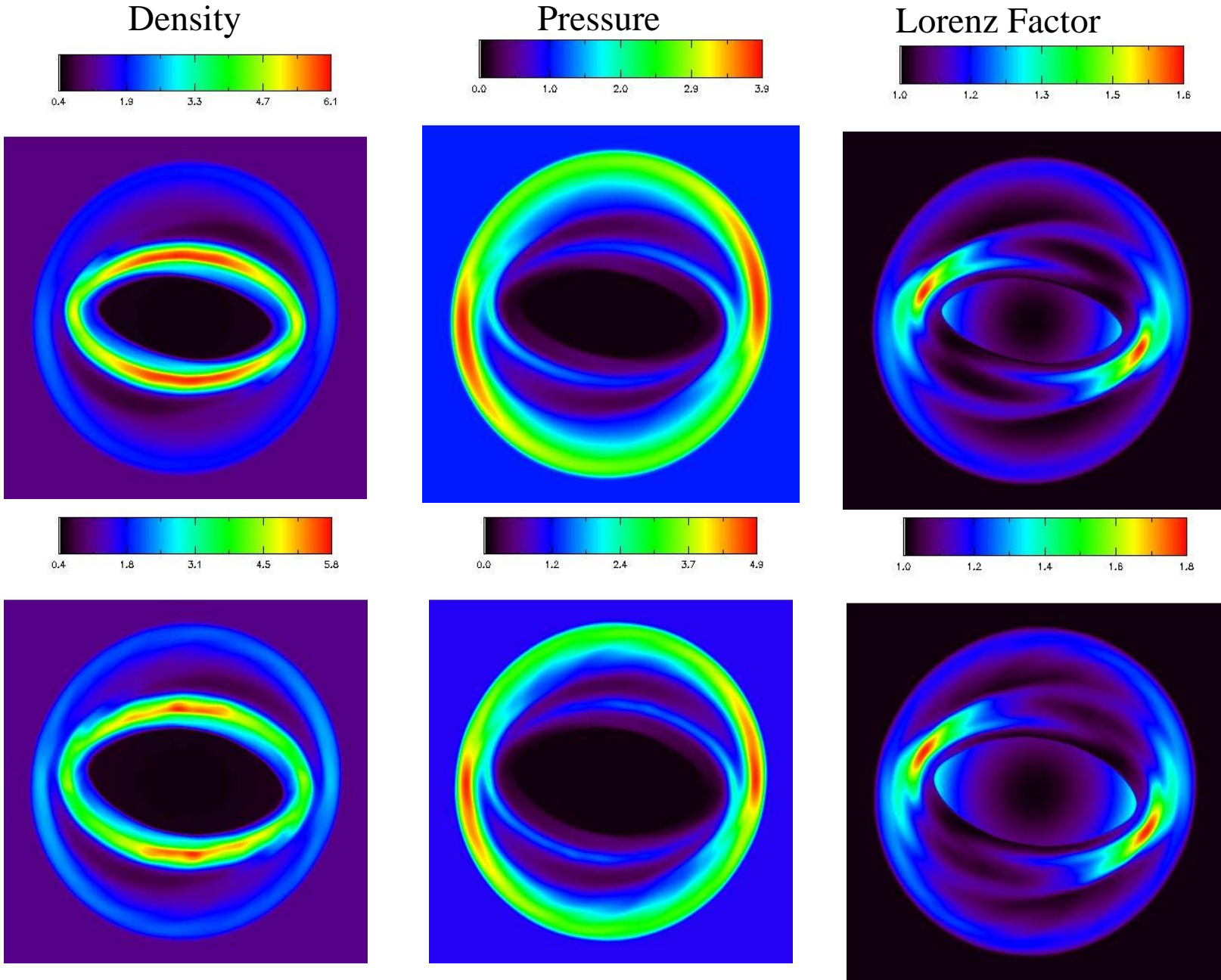
Run with a CFL of 0.6. Near-infinite blast wave propagating through a magnetic plasma with $\beta=0.001$.

Accurate div-free propagation of B-field also gives better **pressure positivity**. (\log_{10} of density and pressure shown.)



RMHD Rotor Problem in 2D : A Case Study with Increasing Lorenz

Factor



$\gamma = 10$

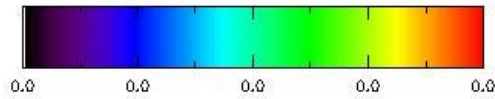
$\gamma = 30$

With J. Kim

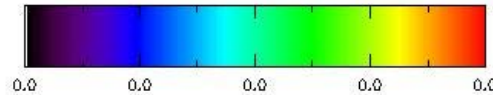
RMHD Blast Problem in 3D

Nearly-Infinite Strength RMHD Blast problem in low plasma- β medium.

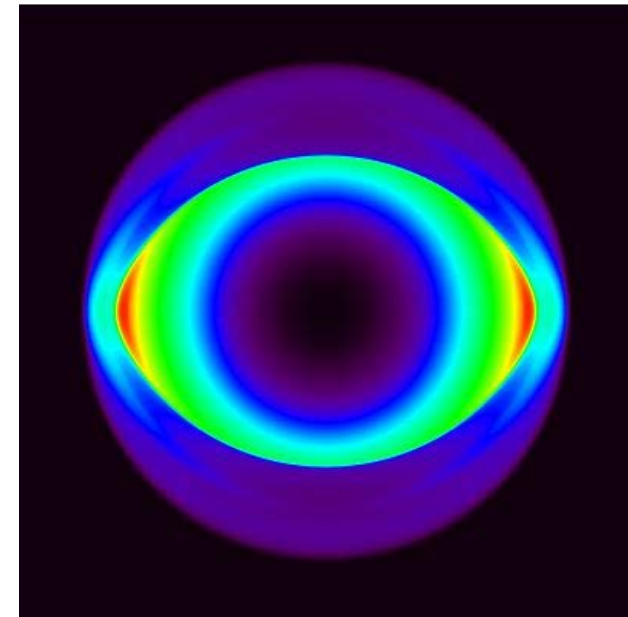
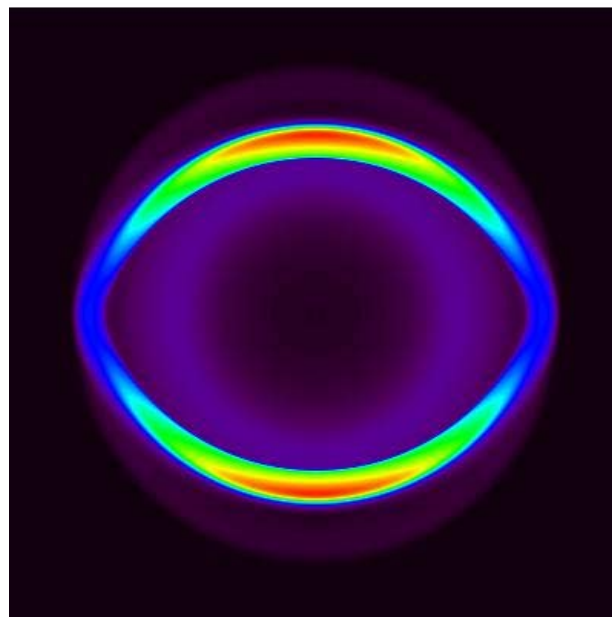
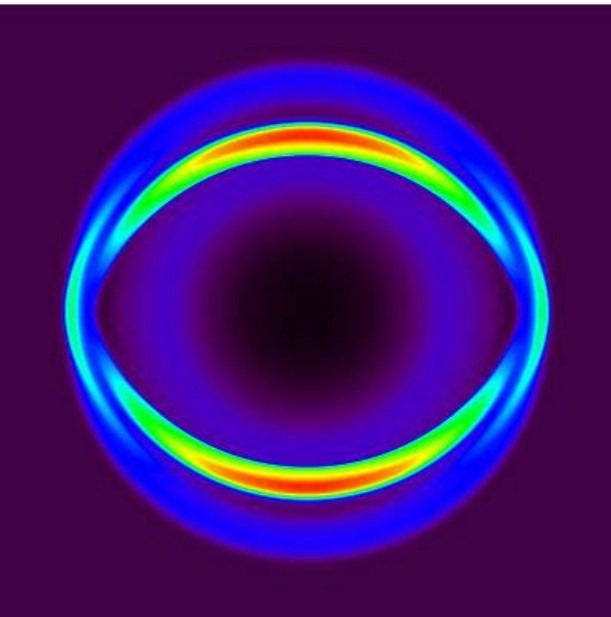
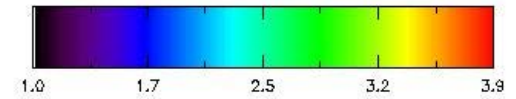
Density



Pressure



Lorenz Factor



VI) Conclusions

- 1) Genuinely **Multidimensional (MuSIC) Riemann Solvers** presented.
Input : multiple states in 2D. **Output**: 1 resolved state + 2 numerical fluxes. Any 1D RS can be used as a building block.
- 2) Addressed all the issues with **introducing self-similar sub-structure in the strongly-interacting state**. It can propagate at any orientation relative to the mesh and provide reduced dissipation.
- 3) All the self-similar equations needed for the formulation are presented as explicit, **computer-implementable, closed-form formulae**. This makes the present MuSIC RS technology **very accessible**.
- 4) The process of obtaining the **numerical fluxes explicitly** is presented.
- 5) **Larger CFL numbers** possible compared to conventional RS-based technology.
- 6) **Predictor-Corrector like ADER-WENO** formulation for any order, **cost-competitive implementation** is presented.

- 7) Much more **isotropic propagation of flow features** demonstrated for hydro, MHD and RMHD flows.
- 8) There is **no need to double dissipation** when evaluating electric fields in MHD calculations.
- 9) The 2D MuSIC RS also helps out with retaining **pressure positivity** in MHD and RMHD problems with **very low plasma- β** .
- 10) Demonstrated value of the MuSIC Riemann solver for **ALE meshes**.
- 11) It is very satisfying that the **MuSIC RS approximates the multid. RP** quite well with only a few terms in the series expansion.

More At: <http://physics.nd.edu/people/faculty/dinshaw-balsara>

Please also see the website for my book:

<http://www.nd.edu/~dbalsara/Numerical-PDE-Course>

Thanks for your attention!

Dinshaw S. Balsara
(dbalsara@nd.edu) Univ. of Notre Dame

<http://physics.nd.edu/people/faculty/dinshaw-balsara>

<http://www.nd.edu/~dbalsara/Numerical-PDE-Course>